

1    **Automated literature mining and hypothesis generation through a network of**  
2    **Medical Subject Headings**  
3

4    Stephen Joseph Wilson<sup>1</sup>, Angela Dawn Wilkins<sup>2,4</sup>, Matthew V. Holt<sup>1</sup>, Byung Kwon Choi<sup>3</sup>,  
5    Daniel Konecki<sup>4</sup>, Chih-Hsu Lin<sup>4</sup>, Amanda Koire<sup>4</sup>, Yue Chen<sup>5</sup>, Seon-Young Kim<sup>2</sup>, Yi Wang<sup>1</sup>,  
6    Brigitta Dewi Wastuwidyaningtyas<sup>2</sup>, Jun Qin<sup>1</sup>, Lawrence Allen Donehower<sup>3</sup>, and Olivier  
7    Lichtarge<sup>1,2,3,4,6,7,\*</sup>  
8

9    <sup>1</sup>Department of Biochemistry and Molecular Biology, Baylor College of Medicine, Houston, TX  
10    77030, USA

11    <sup>2</sup>Department of Molecular and Human Genetics, Baylor College of Medicine, Houston, TX  
12    77030, USA

13    <sup>3</sup>Department of Molecular Virology & Microbiology, Baylor College of Medicine, Houston, TX  
14    77030, USA

15    <sup>4</sup>Department of Quantitative and Computational Biosciences, Houston, TX 77030, USA

16    <sup>5</sup>Department of Molecular and Cellular Biology, Houston, TX 77030, USA

17    <sup>6</sup>Computational and Integrative Biomedical Research Center, Baylor College of Medicine,  
18    Houston, TX 77030, USA

19    <sup>7</sup>Department of Pharmacology, Baylor College of Medicine, Houston, TX 77030, USA

20    \*To whom correspondence should be addressed: (713) 798-5646, lichtarge@bcm.edu  
21

22    **Keywords:** Hypothesis Generation / Literature Discovery / Medical Subject Headings / Methods  
23    and Resources

24 **ABSTRACT**

25 The scientific literature is vast, growing, and increasingly specialized, making it difficult to  
26 connect disparate observations across subfields. To address this problem, we sought to develop  
27 automated hypothesis generation by networking at scale the MeSH terms curated by the National  
28 Library of Medicine. The result is a Mesh Term Objective Reasoning (MeTeOR) approach that  
29 tallies associations among genes, drugs and diseases from PubMed and predicts new ones.  
30 Comparisons to reference databases and algorithms show MeTeOR tends to be more reliable. We  
31 also show that many predictions based on the literature prior to 2014 were published  
32 subsequently. In a practical application, we validated experimentally a surprising new  
33 association found by MeTeOR between novel Epidermal Growth Factor Receptor (EGFR)  
34 associations and CDK2. We conclude that MeTeOR generates useful hypotheses from the  
35 literature (<http://meteor.lichtargelab.org/>).

36 **AUTHOR SUMMARY**

37 The large size and exponential expansion of the scientific literature forms a bottleneck to  
38 accessing and understanding published findings. Manual curation and Natural Language  
39 Processing (NLP) aim to address this bottleneck by summarizing and disseminating the  
40 knowledge within articles as key relationships (e.g. TP53 relates to Cancer). However, these  
41 methods compromise on either coverage or accuracy, respectively. To mitigate this compromise,  
42 we proposed using manually-assigned keywords (MeSH terms) to extract relationships from the  
43 publications and demonstrated a comparable coverage but higher accuracy than current NLP  
44 methods. Furthermore, we combined the extracted knowledge with semi-supervised machine  
45 learning to create hypotheses to guide future work and discovered a direct interaction between  
46 two important cancer genes.

47  
48  
49

## 50 INTRODUCTION

51 It is difficult to keep abreast of new publications. Currently, PubMed contains over 28 million  
52 papers (<http://www.ncbi.nlm.nih.gov/pubmed>)—3 million more than three years ago. This steady  
53 accumulation of findings gives rise to a large number of latent connections that Literature-Based  
54 Discovery (LBD) seeks to systematically recognize and integrate [1], such as Swanson's original  
55 finding linking fish oil to the treatment of Raynaud's disease [2]. Since this original analysis,  
56 LBD has been extensively replicated, automated and expanded [3-10], leading to new patterns of  
57 inference – e.g. locating opposing actions of a disease and a drug on given physiological  
58 functions [11] – and to new discoveries [12]. Successes include the automated discovery of  
59 protein functions [13, 14] and of the genetic bases of disease [15, 16], as well as the stratification  
60 of patient phenotypes [17] and outcomes [18].

61 A limitation of LBD, however, is its dependence on knowledge extraction. It either relies  
62 on human curation, which is not scalable, or on comprehensive text-mining, for which  
63 algorithms are less accurate [19, 20]. One of the largest curated multi-modal biomedical data  
64 sources is the Comparative Toxicogenomics Database (CTD). CTD relied on five full-time  
65 biocurators to curate 70-150 articles a day [21] and gather drug-gene, drug-disease, and gene-  
66 disease associations from 88,000 articles, or about 0.3% of PubMed. By contrast, Natural  
67 Language Processing (NLP) combines semantic analysis of word meaning with syntactic  
68 knowledge of word grammar to break down sentences into biomedical associations. It  
69 automatically extracts knowledge from the entire literature without human supervision [22, 23],  
70 and it is improving [24] but still much less accurate than human curation [23, 25].

71 To combine the benefits of human curation with the scalability of text-mining, we note  
72 that an exhaustive manual curation of PubMed articles already exists. In order to facilitate article  
73 indexing and retrieval, curators at the National Library of Medicine assign Medical Subject  
74 Headings (or MeSH terms) and Supplemental Concept Records (SCR) to every PubMed article.  
75 These terms (<https://www.ncbi.nlm.nih.gov/pubs/factsheets/mesh.html>) summarize key biomedical  
76 concepts for each paper, and to expand coverage and refine relevance, they are revised annually  
77 (or daily for SCRs) [26] (<https://www.ncbi.nlm.nih.gov/pubs/factsheets/mesh.html>). The co-  
78 occurrence of MeSH terms with text-mined gene names was used to cross-reference genes and  
79 predict diseases that shared disease characteristics and chromosomal locations [27, 28].  
80 Unfortunately, this was dependent on NLP for the identification of the genes (due to a reported

81 low-coverage of gene MeSH terms in 2003) and required additional databases of information for  
82 chromosomal locations. Another study suggested that weighting MeSH terms (TF\*IDF) was  
83 beneficial [29]. More recently, MeSH term co-occurrence was analyzed with various  
84 unsupervised and supervised techniques to make retrospective and prospective hypothesis [30]  
85 that predicted future associations between MeSH terms accurately [30]. This approach used all  
86 MeSH terms, including broad terms such as “Proteins”, but not SCR. Unfortunately, the  
87 individual terms were not mapped to canonical gene and drug terms, such as HGNC[31] and  
88 PubChem [32] identifiers restricting comparisons to curated datasets. Overall, the use MeSH  
89 terms in LBD has been limited in a few applications with regards to gene accuracy/coverage,  
90 selection and mapping of MeSH terms, and comparisons to curated datasets.

91 To improve on the generality, scalability and accuracy of these approaches we sought to  
92 comprehensively use MeSH terms for genes, to add the information from SCRs, and to perform  
93 thorough comparisons against biological standards and among the latest NLP methods. We also  
94 developed a robust unsupervised link prediction algorithm and experimentally tested a top  
95 prediction. The result is a literature-derived network called MeTeOR (the MeSH Term Objective  
96 Reasoning approach), which represents gene-drug-disease relationships exclusively from MeSH  
97 term and SCR co-occurrence. We show below that MeTeOR supplements knowledge from  
98 reference databases and more accurately recovers known relationships than traditional text-  
99 mining. Pairing the MeTeOR network with Non-Negative Matrix Factorization (NMF), an  
100 unsupervised machine learning algorithm, significantly improved LBD performance.

101

## 102 **RESULTS**

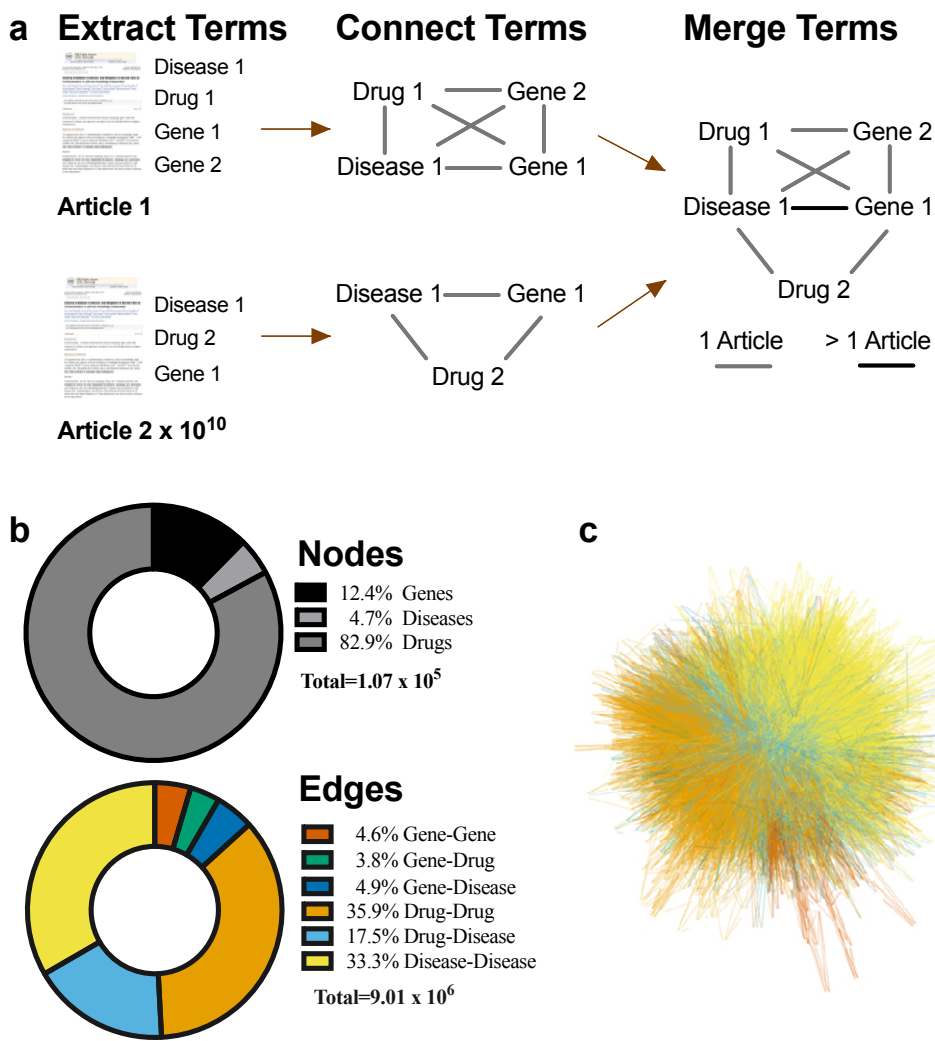
### 103 **Developing a literature-based network from MeSH terms**

104 In order to represent published biological associations among genes, drugs, and diseases,  
105 we took the Medical Subject Headings (MeSH) and Supplemental Concept Records (SCR)  
106 assigned to more than 21,531,000 MEDLINE articles by the National Library of Medicine  
107 (NLM) (**Supplemental Fig. 1**). MeSH terms facilitate indexing and searching, and SCR terms  
108 were created to identify drugs too numerous to be directly added as MeSH terms. (SCR terms  
109 also represent diseases and genes, among other topics.) Each distinct MeSH and SCR term  
110 became one of 276,000 nodes with 286 million term-article relationships. Nodes that co-occurred  
111 in a paper were fully connected into a clique for each article, and cliques were joined when they

112 shared nodes across articles (**Figure 1A**). This generated a single network with 129 million term-  
113 term non-overlapping edges in which the number of articles that gave rise to a given pair of  
114 nodes measures the confidence of their association. Of these nodes, 39% mapped to 89,000  
115 drugs, 4,800 diseases, and 13,000 genes, forming 9 million edges. The network consisted  
116 primarily of genes (12%) and drugs (82%), but, given the focus of much biomedical research on  
117 disease, 56% of edges contained a disease (**Figure 1B**). As articles get added to MEDLINE, the  
118 network can be updated as soon as they have been annotated by the NLM.

119 This network was too visually dense to interpret, even when focusing on only high-  
120 confidence relationships (conf. >200 articles, degree >3) (**Figure 1C**). The complexity of the  
121 network and the presence of complete cliques at the article-level led us to evaluate the network's  
122 topology. When limited to genes, drugs, and diseases, MeTeOR best fits a scale-free network  
123 with a power-law distribution of node degrees, where  $\gamma \approx 1.34$  ( $p$ -value  $\ll 10^{-35}$  compared to log-  
124 normal and exponential distributions; **Supplemental Fig. 2**) [33] and some nodes have a much  
125 higher node degree, i.e. greater connectivity. The presence of such hubs is a common feature of  
126 real-world networks [34]. MeTeOR thus condenses PubMed knowledge into a computable and  
127 well-structured network that is amenable to analysis by established network algorithms.

Wilson - Figure 1



128

129 **Figure 1. MeSH terms can provide a reliable approximation of biomedical knowledge in**  
130 **the literature.** A) MeSH terms are taken from an article, connected into a clique, and then  
131 merged by nodes across over 22 million articles in PubMed. Any associations that overlap  
132 between articles are considered to have greater confidence. B) Graphical representation of the  
133 proportion of nodes for each entity type and the percentage of edges per association type. C) The  
134 MeTeOR network as a whole is formidable, despite the exclusion of all edges with a confidence  
135 of less than 200 articles.

136

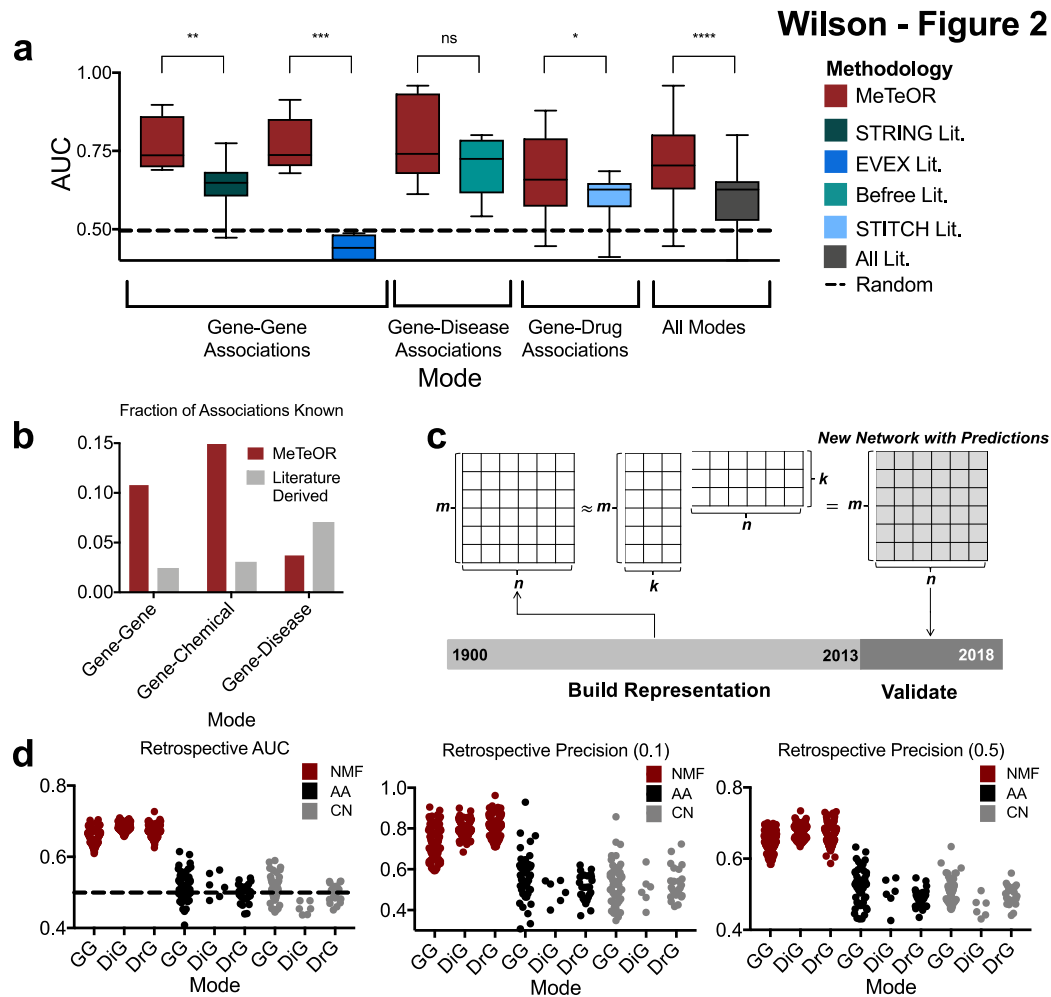
137 **MeTeOR outperforms literature-derived databases in number and reliability of**  
138 **associations**

139 To assess the coverage and quality of MeTeOR, we compared it first with specialized,

140 gold-standard databases. MeTeOR tallies about twenty percent more gene-gene associations than  
141 BIOGRID low-throughput associations (177,000 vs 147,000; **Supplemental Fig. 3**). More  
142 impressively, MeTeOR contains 16.4 and 15.9 fold more gene-disease and gene-drug  
143 associations than CTD and DGIdb respectively. Yet despite these gains in associations,  
144 MeTeOR overlapped each of these control databases to the same extent that they overlapped  
145 each other (**Supplemental Fig. 3**).

146 MeTeOR also proved as reliable as these databases, preferentially recovering the high-  
147 quality reference annotations over novel information. In other words, when MeTeOR  
148 associations were ordered by confidence (the number of supporting articles), the area under the  
149 Receiver Operating Characteristic (ROC) curves (AUC) averaged 0.71 for all references (**Figure**  
150 **2A**). The average precision at 10% recall was 0.85 and at 50% recall was 0.73. (**Supplemental**  
151 **Fig. 4**).

152 We next compared MeTeOR to the literature-mining methods STRING-Literature [35],  
153 EVEX [22], BeFree [36], and STITCH-Literature [37]. These methods extract only one type of  
154 association from the literature—gene-gene, gene-disease, or gene-drug, respectively—and  
155 MeTeOR outperformed each of them across all references, except the BeFree method on the  
156 CTD reference. MeTeOR also outperformed all methods combined, both with and without the  
157 poor-performing EVEX (**Figure 2A**). It is worth noting that MeTeOR contained several-fold  
158 more novel associations than these other text-mining tools (**Figure 2B**), even though it has  
159 roughly the same order of magnitude of overlap with the references (**Supplemental Fig. 3**).  
160 These data show that MeTeOR mines more gene-gene, gene-disease, and gene-chemical  
161 associations than are found in our reference databases, while simultaneously recovering high-  
162 quality references better than the state-of-the-art text-mining tools.



163

164 **Figure 2. MeTeOR reliably recovers known associations and predicts new biomedical**  
 165 **knowledge.** A) MeTeOR was compared with appropriate algorithms using the area under the  
 166 Receiver Operating Characteristic (ROC). All tests were done with bootstrapping to give a  
 167 confidence range and to balance the positives and negatives. The literature-derived algorithms  
 168 were STRING-Literature, EVEX, STITCH-Literature, and BeFree for genes, genes, drugs, and  
 169 diseases, respectively. From left to right, the *p*-values comparing MeTeOR to the literature-  
 170 derived networks were 0.0076 (*t*=3.707, *df*=7), 0.0001 (*t*=7.822, *df*=7), 0.0432 (*t*=2.125, *df*=26),  
 171 0.094 (*t*=2.145, *df*=5), <0.0001 (*t*=5.172, *df*=48). Excluding EVEX, MeTeOR's difference from  
 172 the literature-derived networks is still significant *p*-value<0.0005 (*t*=3.79, *df*=40). B) MeTeOR  
 173 contained more known associations than the comparable algorithms in two of the three cases,  
 174 and possessed more overall (17% vs 12%). C) In order to test the ability of the network to  
 175 reliably predict biomedical associations, we performed a time-stamped, or retrospective, study.

176 The product of the latent matrices W and H from pre-2014 data resulted in a new network with  
177 predictions. Predictions were validated if they were borne out in the literature between 2014 and  
178 2018. D) The area under the ROC was calculated for MeTeOR gene-gene, gene-disease, and  
179 gene-drug associations based on Nonnegative Matrix Factorization (NMF) predictions being  
180 present in the 2018 network. These were compared against predictions from two naïve  
181 predictors, Common Neighbors (CN) and Adamic/Adar (AA). E) Positive predictive values  
182 (precision) were calculated at 10% and 50% recall. (\*  $p<0.05$  , \*\*  $p<0.01$ , \*\*\*  $p<0.001$ ).  
183

#### 184 **Testing MeTeOR predictions with retrospective analyses**

185 We next tested MeTeOR's ability to predict novel associations among genes, diseases,  
186 and drugs. Kastrin et al. recently tested both supervised and unsupervised link prediction  
187 methods on a MeSH co-occurrence network of 27,000 entities and found they could generate  
188 reliable hypotheses [30]. We hoped to build upon this attempt by using a more advanced link  
189 prediction method, Non-negative Matrix Factorization (NMF), with our greater number of  
190 entities (totaling 101,000). Often used in biology [38, 39], NMF is a semi-supervised machine  
191 learning algorithm that determines missing associations in a graph by decomposing it into a  
192 product of matrices [40]. Therefore, we tested the predictive power of the top two unsupervised  
193 algorithms from Kastrin et al. [30], Adamic/Adar (AA) and Common Neighbors (CN), and NMF  
194 in a retrospective study.

195 Here, we used cross-validation to estimate the number of features for each part of the  
196 NMF decomposed matrix (**Figure 2C, Supplemental Table 1**). When we applied NMF, we used  
197 a representation of MeTeOR derived solely from publications up to and including the year 2013  
198 to test whether MeTeOR's predicted associations would be confirmed by appearing in literature  
199 published between 2014 and 2018. The median AUCs of gene-gene, gene-disease, and gene-drug  
200 associations were 0.65, 0.69 and 0.67, respectively (**Figure 2D, left**), while the median precisions  
201 at 10% recall (the top 10% of the highest-confidence associations) were 0.75, 0.79, and 0.81,  
202 respectively and 0.65, 0.68, 0.67 at 50% recall (**Figure 2D, middle and right**). Moreover, using  
203 AA and CN results in random predictive power, or AUCs at 0.5 (AA: 0.53, 0.50, 0.49; CN: 0.51,  
204 0.46, 0.50; for gene-gene, gene-disease, and gene-drug median AUCs, respectively). It is  
205 important to note that the AA and CN predictions are distinct from previous attempts [30] in that  
206 the network excludes many general MeSH terms, includes SCRs, and is split into separate

207 association modes. Due to NMF's reliable and higher performance, we chose it for subsequent  
208 analyses. These data show that the hypothetical associations among genes, drugs, and diseases  
209 produced by MeTeOR are likely to be confirmed in subsequent literature, especially those with  
210 the best confidence.

211 We investigated some of the top time-stamped associations in more detail in order to  
212 confirm the biological relevance of these predictions. To date, the literature has provided  
213 supporting evidence for 19, 17, and 18 out of the top 20 hypotheses from gene-gene, gene-  
214 disease, and gene-drug associations, respectively (**Supplemental Data File 1**). For example, a  
215 top predicted gene-gene association, based solely on the literature published up to and including  
216 2013, was between the human MeSH terms for *MSX1* and *CXCR4*. In 2017, a paper was  
217 published showing that both *MSX1* and *CXCR4* independently regulate the motility and  
218 development of a population of highly migratory cells, known as primordial germ cells which  
219 give rise to eggs and sperm migration [41], and confirming MeTeOR's hypothesis that these  
220 genes are linked in a biologically meaningful manner. To demonstrate a more complex, specific  
221 and novel prediction, MeTeOR predicted an association between *PTEN* and glaucoma based on  
222 pre-2013 literature. In the beginning of 2018, a paper was published demonstrating that  
223 microRNA MiR-93-5p, which targets *PTEN*, regulates NMDA-induced autophagy in glaucoma.  
224 Several other papers published after 2014 [42, 43] also suggested some role for *PTEN* in  
225 glaucoma. MeTeOR also predicted an association between *GLI1* and multiple myeloma, and in  
226 2017, Alu-dependent RNA editing of *GLI1* was shown to promote malignant regeneration in  
227 multiple myeloma [44].

228 There were also some more complex indirect three-way associations (ex. gene-disease-  
229 gene). For example, the top gene-gene prediction is between *CD27* and *CXCR4*. This prediction  
230 makes sense in the context of the human immunodeficiency virus (HIV), where HIV-1 variants  
231 use *CXCR4* to infect T cells, and through this process, HIV depletes both naïve and *CD27<sup>+</sup>*  
232 memory T cells [45]. This demonstrates the predictive power of the network by highlighting a  
233 complex gene-disease-gene relationship (*CXCR4* – HIV – *CD27*). Another example is between  
234 *WT1* and *HLA-B*. The *WT1* protein has been chosen as an immunologic target by a National  
235 Cancer Institute initiative [46], and this year, a phase 2 clinical trial showed a *WT1* vaccine that  
236 is effective in Acute Myeloid Leukemia with predicted binding on *HLA-B\*15:01*, *HLA-*  
237 *B\*39:01*, *HLA-B\*07:02*, and *HLA-B\*08*, *HLA-B27:05* in addition to *HLA-A\*02* [47]. These

238 MeTeOR predictions suggests that further investigation is warranted and highlights the ability of  
239 the network to suggest complex gene–disease–gene relationships.

240 Though these hypotheses are only a small sample of all MeTeOR-identified links, they  
241 illustrate the power and range of MeTeOR’s NMF predictions.

242

### 243 **MeTeOR identifies known and novel *EGFR* associations**

244 To illustrate how MeTeOR might be used, we focused on Epidermal Growth Factor  
245 Receptor (EGFR) as a test case. EGFR is a well-studied protein involved in various aspects of  
246 carcinogenesis [48], and we hypothesized that MeTeOR would be able to extract known and  
247 novel associations from the wealth of extant literature.

248 We first needed to understand EGFR’s known and verifiable associations. MeTeOR  
249 found 1064 genes connected to EGFR via MeSH terms in at least one article, 467 genes in at  
250 least two articles, and 97 genes in at least ten articles. Assuming that associations made by more  
251 articles would be more robust, we compared the MeTeOR-ranked list of 1064 gene-EGFR  
252 associations against the MSIGDB pathway standard used in Figure 2.

253 MeTeOR recovered pathway information better than the text-mining algorithm EVEX  
254 (overall  $AUC_{MeTeOR}$  of 0.88 vs  $AUC_{EVEX}$  of 0.69; **Figure 3A**). MeTeOR’s initial recall was also  
255 superior, as indicated by the Precision-Recall curve (**Figure 3B**). Finally, MeTeOR was overall  
256 more accurate than STRING Literature ( $AUC_{STRING}$  of 0.75), although in the initial recall,  
257 STRING did better, likely because it weighs confidence based on KEGG pathway information  
258 [49] (**Figure 3B**).

259 We then sought to evaluate MeTeOR’s likelihood of generating false positives. Reliance  
260 on MeSH terms could, for example, create a spurious link between EGFR and another gene if the  
261 publication is a review article that mentions another gene without actually proposing a  
262 relationship with EGFR. We noticed that 12 of the top 20 genes MeTeOR associated with EGFR  
263 did not appear in MSIGDB pathway standard (**Figure 3C, Supplemental Fig. 5**). We therefore  
264 compared these top 20 genes against experimental associations derived from public sources  
265 (aggregated in STRING-Experimental). The STRING-Experimental dataset (STRING-EXP),  
266 which showed that 13 out of the top 20 genes physically interact with EGFR (**Figure 3C**),  
267 revealed that six of the twelve genes missed by MSIGDB are actually valid (**Supplemental Fig.**  
268 **5**). This brought the number of genes with curated evidence from MSIGDB pathways or

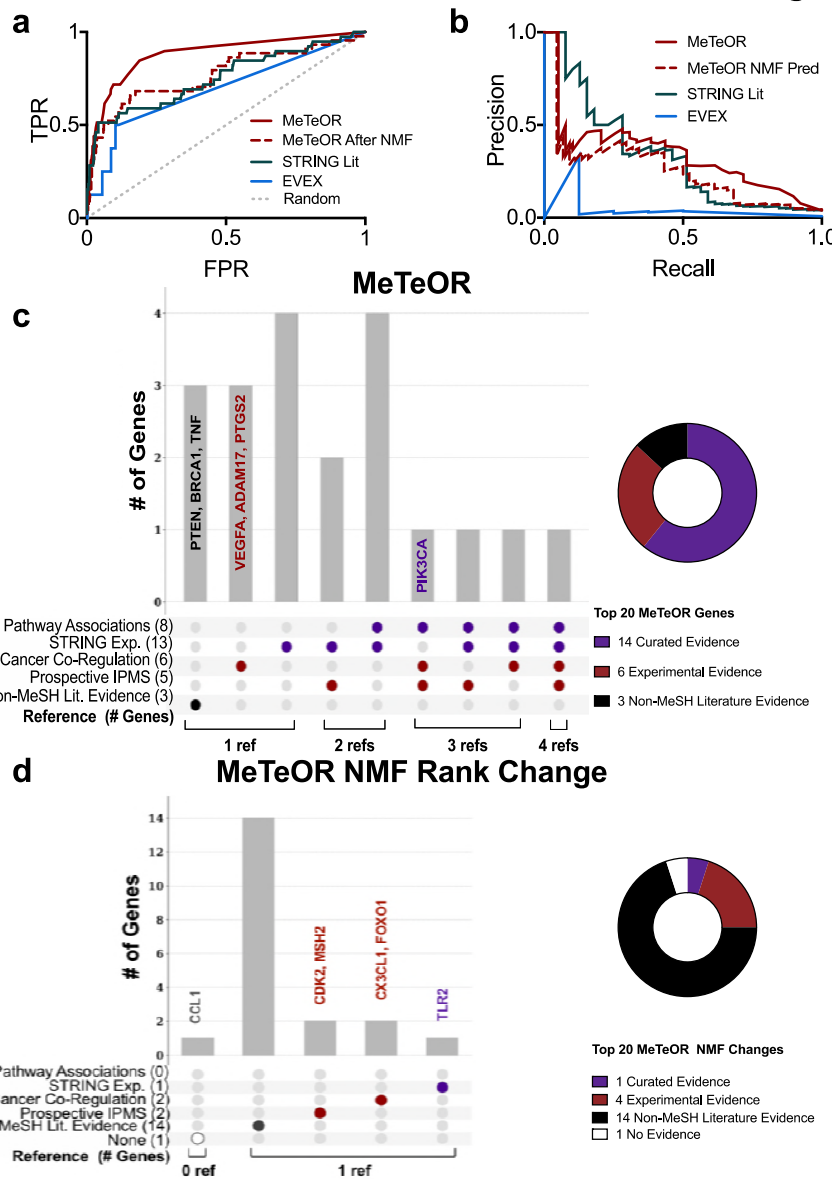
269 STRING from eight up to 14 (**Figure 3D**). For the remaining six genes, we pursued two analyses  
270 based on experimental evidence, one involving pan-cancer RNA-seq data (from 8768 TCGA  
271 patients [50], see Online Methods) and the other a prospective, unbiased high-throughput Mass  
272 Spectrometry experiment.

273 We calculated the co-expression of all genes in 20 TCGA cancer types and thresholded  
274 them by the correlation co-efficient. The mRNA levels of three of the six putative “false  
275 positive” genes correlated with EGFR mRNA levels ( $|r| > 0.25$ , Online Methods). For example,  
276 PTGS2 was not associated by pathways but was co-expressed with a q-value  $<< 0.01$ ,  $r = 0.29$ .  
277 This appears to be a biologically relevant relationship insofar as both PTGS2 and EGFR are  
278 prognostic biomarkers for several of the same cancers [51, 52], and PTGS2 expression levels can  
279 predict the efficacy of treatments that act on EGFR [53]. EGFR associations with the other two  
280 genes (*VEGFA* and *ADAM17*) appear equally valid (**Supplemental Data File 2**).

281 For the high-throughput Immuno-Precipitation Mass Spectrometry (IPMS), we pulled  
282 down EGFR at several time-points after stimulation with Epidermal Growth Factor (EGF) in  
283 order to obtain a snapshot of proteins binding with EGFR in a functional context (**Supplemental**  
284 **Fig. 6, Supplemental Data File 3**). IPMS showed that five of the 20 genes were associated with  
285 EGFR, though all were also associated with MSIGDB pathways or STRING. One of these five  
286 was *PIK3CA*, which possesses links through pathway knowledge, cancer co-regulation and the  
287 IPMS; it is frequently co-mutated with EGFR [54] and known to interact with other PI3K  
288 subunits (PIK3CB [55] and PIK3R1 [56]) [57].

289 In the end, just three genes (*PTEN*, *BRCA1*, and *TNF*) remained putative false positives  
290 (**Figure 3C**). All three, however, have some degree of literature support, denoted as non-MeSH  
291 literature evidence because it is manually curated and not originating from MeSH terms  
292 (**Supplemental Data File 2**). For example, *PTEN* is often lost in cancers with *EGFR* gains [58]  
293 and the EGFR/PI3K/PTEN/Akt/mTORC1/GSK-3 pathway causes malignant transformation,  
294 drug resistance, metastasis, and prevention of apoptosis [59]. Thus, even the apparent false  
295 positives in the top 20 associations seem to warrant investigation.

### Wilson - Figure 3



296

297 **Figure 3. MeTeOR-identified associations with EGFR and NMF predictions. A)** EGFR  
 298 MeTeOR, STRING-Literature (lit.), and EVEEX literature associations are compared against  
 299 pathway-level interactions, with AUCs of 0.88, 0.75, and 0.69, respectively. **B)** In the precision  
 300 recall curve, MeTeOR's initial false positive rate is lower than that for EVEEX, but higher than  
 301 that for STRING-Lit. **C)** The overlap of the top 20 MeTeOR Genes with curated (MSIGDB and  
 302 STRING Experimental) and experimental (Cancer Co-Expression and Prospective  
 303 ImmunoPrecipitation Mass Spectrometry) evidence. Genes that did not fall into these categories  
 304 were verified in the literature manually or determined to have no evidence (Supplemental Data  
 305 File 2). Genes possessing experimental evidence and/or one or two references of support, which

306 are of particular interest, are written on the chart. Genes classified with Curated Evidence have at  
307 least curated, with the possibility of Experimental or Non-MeSH Literature Evidence, with  
308 Experimental Evidence having at least Experimental. **D)** The top 20 ranked genes by their  
309 difference from MeTeOR's rankings to their rankings after NMF were also compared against the  
310 same references. All but one of the genes (CCL1) possessed some evidence.

311

### 312 **MeTeOR's automated hypothesis generation predicts new EGFR associations**

313 Although the success of MeTeOR's retrospective associations is reassuring, the real test  
314 of MeTeOR's utility to the scientific community is whether it can reveal unexpected and  
315 valuable biological hypotheses that merit experimental validation. We therefore used EGFR as a  
316 test case again, but instead of using MeTeOR's raw associations, this time we evaluated its Non-  
317 Negative Matrix Factorization (NMF) predictions. These were ranked by their difference from  
318 MeTeOR's rankings, such that:  $NMF\ Rank\ Change = MeTeOR\ Rank - MeTeOR\ NMF\ Rank$ ,  
319 where MeTeOR Weight>2 limits arbitrarily large ranks from genes that initially had little to no  
320 evidence (**Supplemental Data File 4**).

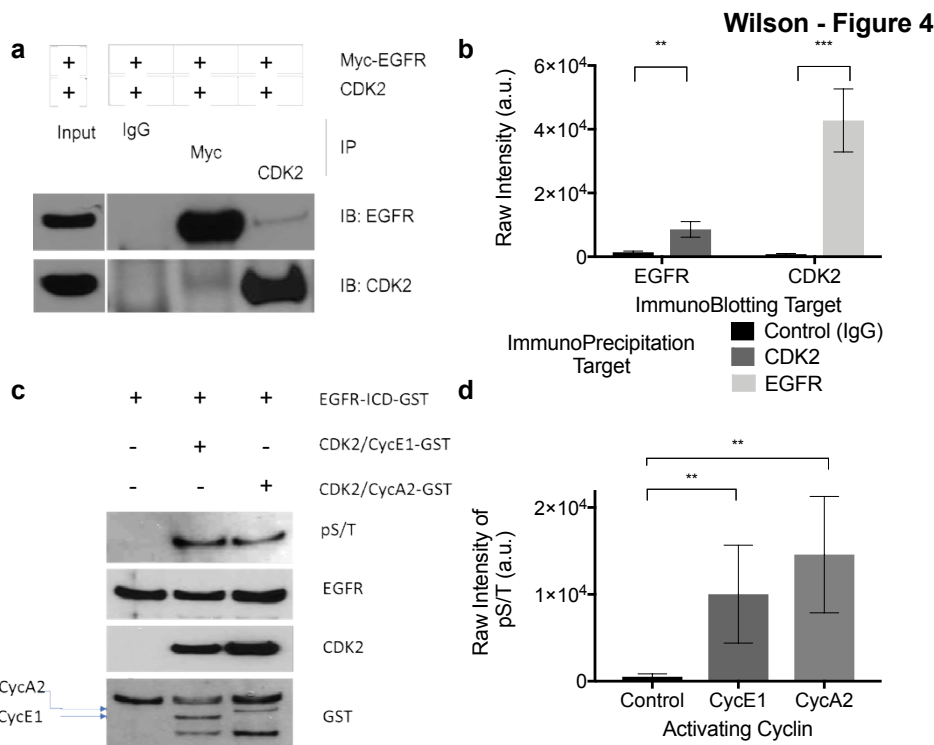
321 Controlled against MSIGDB pathway associations, all 20 predictions were putative “false  
322 positives” and only one possessed STRING-Experimental evidence (TLR2) (**Figure 3D**). This  
323 demonstrates the effectiveness of the NMF Rank Change at highlighting novel predictions. Yet,  
324 of the 19 unproven associations, two were co-expressed in cancer (CX3CL1 and FOXO1) and  
325 two were supported by our IPMS evidence (CDK2 and MSH2) (**Supplemental Fig. 5**). Of the  
326 remaining fifteen genes, all except CCL1 had non-MeSH literature support (**Figure 3D**;  
327 **Supplemental Data File 2**), underscoring the quality of NMF Rank Change predictions.

328 To narrow down candidates for experimental validation, we focused on CDK2 and  
329 MSH2, the proteins for which we had IPMS evidence (**Figure 3D**). Cyclin-dependent kinase 2  
330 (CDK2) seemed the most biologically promising: like EGFR, CDK2 is directly involved in the  
331 cell cycle and cell growth, and it has a similar kinase domain to CDK1, which phosphorylates  
332 EGFR *in vitro* [60]. Furthermore, in apoptosis and senescence, CDK2 translocates to the  
333 cytoplasm with Cyclin A [61] or Cyclin E [62], and under these conditions, an activated CDK2  
334 might bind to and phosphorylate EGFR.

335 To determine whether CDK2 and EGFR directly interact in a biologically relevant  
336 manner, we transfected human embryonic kidney cells with expression vectors for both proteins.

337 Co-immunoprecipitation demonstrated that CDK2 and EGFR formed stable protein-protein  
338 interactions (**Figure 4A, B**). Next, we incubated purified EGFR protein by itself or with CDK2,  
339 along with either its interaction partner Cyclin A2 or Cyclin E1. We found that, *in vitro*, both  
340 Cyclin A and Cyclin E activate CDK2 to phosphorylate EGFR's intracellular regulatory portion  
341 (**Figure 4C, D**) but not to phosphorylate the extracellular portion (**Supplemental Fig. 7**). *In*  
342 *silico* prediction with GPS [63] identified several residues (752, 847, 991, 1026, 1032, and 1153)  
343 as possible sites of intracellular EGFR phosphorylation by CDK2 (**Supplemental Fig. 8**). It is  
344 worth noting that Residue 1026 was previously shown to be phosphorylated by CDK1 [60].

345 This interaction is rather surprising because CDK2 has never been shown to interact with  
346 EGFR. Yet our data indicate that CDK2 directly phosphorylates EGFR, and they bind to one  
347 another *in vivo*. MeTeOR's automated hypothesis-generation thus produced many validated  
348 biological hypotheses, and in the case of CDK2 has revealed an unexpected and valuable  
349 biological insight.



350  
351 **Figure 4. CDK2 phosphorylates EGFR, as predicted by MeTeOR.** A, B) The western blot of  
352 the *in vivo* reciprocal pull-down of EGFR and CDK2 provided evidence of physical interaction  
353 between EGFR and CDK2. HEK293 cells were transfected with myc-tagged WT-EGFR and  
354 WT-CDK2 vectors, and overexpressed EGFR and CDK2 were immunoprecipitated from lysates

355 using anti-myc or anti-CKD2 antibody and quantified over three to five replicates. Mouse IgG  
356 antibody was used as a control. C, D). An *in vitro* kinase assay showed Serine/Threonine  
357 phosphorylation on EGFR by CDK2 with statistically significant levels being generated with  
358 either Cyclin A or Cyclin E activating CDK2. Purified recombinant EGFR-GST was incubated  
359 with recombinant cyclin A2 and cyclin E1 activated CDK2 kinase; quantification on three  
360 replicates for CDK2-Cyclin E and CDK2-Cyclin A was performed with ImageJ (\*  $p$ -  
361 value<0.05, \*\*  $p$ -value<0.01, \*\*\*  $p$ -value<0.001; *in vivo*:  $t$ =6.834,  $df$ =4 for EGFR and  $t$ =3.407,  
362  $df$ =8 for CDK2; *in vitro*:  $t$ =4.961,  $df$ =6 for CycA2 and  $t$ =3.984,  $df$ =6 for CycE1).

363

## 364 **DISCUSSION**

365 Our ability to find interesting relationships among bodies of knowledge separated by time  
366 and disciplinary boundaries is struggling with the ever-increasing size of the scientific literature  
367 [1]. Current tools, such as PubMed and Google Scholar, make it possible to search extant  
368 publications (at least to the extent that the content is available online), but they can reflect and  
369 propagate biases [64]; they cannot evaluate the relative confidence of observations; and they do  
370 not attempt to integrate information into novel hypotheses. Whereas many literature-mining  
371 methods seek to capture semantic and syntactic detail from each paper, we took the opposite  
372 approach, hypothesizing that millions of human-curated keywords could create useful network  
373 structures and that the sheer quantity of data points would wash out erroneous results while  
374 allowing verifiable information to emerge from separate but corroborating studies. Following the  
375 Bag-of-Words representation of knowledge in terms of common, contextual word associations  
376 [65], we focus on the most important facts from each paper embodied by (key) words chosen  
377 from Medical Subject Heading (MeSH) terms. These MeSH terms are readily available and  
378 regularly updated. By representing each article as a clique of MeSH terms, we create networks  
379 that can reveal unsuspected connections across the literature. This effectively converts  
380 unstructured into structured knowledge that, in turn, is amenable to machine learning techniques  
381 to generate new hypotheses.

382 In practice, the MeSH Term Objective Reasoning (MeTeOR) network pooled knowledge  
383 from over 22 million PubMed articles to create a map of relationships among genes, drugs, and  
384 diseases. MeTeOR recovered knowledge from reference databases and revealed many previously  
385 uncharacterized biomedical associations; its performance was on par with or better than domain-

386 specific and state-of-the-art Natural Language Processing (NLP) models for knowledge  
387 extraction. Moreover, hypothesis generation through non-negative matrix factorization predicted  
388 new associations prior to their publication. This predictive efficacy was further demonstrated by  
389 MeTeOR's ability to discern known and novel EGFR interactions more reliably than NLP  
390 algorithms. In particular, MeTeOR predicted an association between CDK2 and EGFR, and we  
391 confirmed and simultaneously suggested the association is a direct physical interaction with  
392 high-throughput IPMS screening. This interaction has implications for biological processes such  
393 as cell cycle, cell growth, and apoptosis as well as disease processes such as tumorigenesis. Both  
394 CDK2 [66] and EGFR [67] are targets of cancer therapies, but previous hints of a relationship  
395 between the two proteins had been attributed to similarities in structural activation [68] or distant  
396 regulatory effects [69]. Our experimental data verified this interaction, which had been latent in  
397 the literature but gone unnoticed. Together, these results demonstrate that the breadth and  
398 redundancy of keyword coverage in the literature compensate for the superficiality of the  
399 information taken from any one article and can accurately represent knowledge across a large  
400 corpus of literature, creating hypotheses that warrant experimental investigation.

401 In the future, MeTeOR can be improved in a number of ways. It could be combined with  
402 orthogonal databases [49] or ontological hierarchies [70] so as to improve the network accuracy  
403 and coverage. Additional relevant keywords, such as the context of an association (e.g.,  
404 regulation, phosphorylation) and MeSH terms for biological processes, therapies, and clinical  
405 variables, could deepen MeTeOR analyses. Labels that convey dates, number of citations,  
406 journal, and other contextual details might provide useful qualifiers for the confidence of  
407 associations. Alternatively, defining the semantic meaning of the relationship may be done  
408 through integration of the SemRep system [71]. Keyword indexing exists in fields outside  
409 biomedicine [72] and could be turned, likewise, into knowledge networks that summarize and  
410 support machine learning over entirely different domains of knowledge. For now, MeTeOR is a  
411 public, reliable source of gene, drug, and disease associations that directly link to PubMed  
412 references, improving accessibility and indexing of the literature, while enabling its use for  
413 hypothesis generation across biology.

414

## 415 **MATERIALS AND METHODS**

416 **Indexing Information to Represent Biomedical Knowledge:** Co-occurrence strengthens the

417 confidence in associations as the number of articles sampled increases [73]. Supplementary  
418 Concepts Records (SCRs) are similar to MeSH terms and cover a wide variety of concepts  
419 including genes, drugs, and diseases. They were used in addition to MeSH terms to supplement  
420 the existing data. All data was obtained using the NCBI eutils tool and a list of all PubMed IDs  
421 associated with a search for Eukaryotes, Bacteria, Viruses, and Archea (~22 million articles). All  
422 proteins were mapped to Entrez ids using supplementary concepts annotations of RefSeq  
423 numbers in the notes section where possible and by symbol or synonym if no RefSeq number  
424 was present. All drugs and diseases were mapped using the MeSH hierarchy as done in previous  
425 works [21, 74], with PubChem CIDs used for drugs and MeSH ids for diseases. In order to  
426 obtain the co-occurrence of these terms, we calculated the dot-product of the term-article  
427 membership matrix. Terms that mapped to the same Entrez ids were summed by edge weights.  
428

429 **Data Visualization:** The MeTeOR network was filtered to only use edges that had a confidence  
430 over 200, and while nodes were made invisible. The weights of each edge represented as the  
431 penwidth for each edge. The format for the network was assembled in NetworkX  
432 (<https://networkx.github.io/>) in python as DOT file, and then the network was visualized using  
433 the sfdp tool of GraphViz (<http://www.graphviz.org/>).

434  
435 **Ground Truth Comparisons:** The network was compared against highly accessed and cited  
436 databases in order to determine if the network contains valid associations between terms. These  
437 comparisons measure the recovery of a reference database based on the ranking of the others  
438 (MeTeOR or a literature-derived source), and the data output is the recovery rate of true positives  
439 (TPR) and false positives (FPR). A true positive was defined as an association present in  
440 MeTeOR that also was present in the ground truth.

441  
442 **Robust Comparisons:** Receiver Operating Characteristic (ROC) plots can lead to inaccurate  
443 representations of the data when there are unbalanced numbers of true and false negatives. In  
444 particular, if there is a space of 100,000 by 100,000 possible associations between drugs and  
445 genes, most of the possible interactions will be True Negatives, making the False Positive Rate  
446 increase extremely slowly according to the formula:

$$447 \quad FPR = \frac{FP}{FP + TN}$$

448 This leads to inflated AUCs. To solve this problem, the number of positives and negatives was  
449 determined, and an approximately equal number of positives and negative were chosen randomly  
450 together up to a hundred times. This was designed to randomly sample for complete coverage of  
451 all positives. Occasionally, the number of positives per iteration was below 100, and in order to  
452 make each iteration more reliable, the number of iterations was decreased. This allowed the  
453 determination of a range of accuracy scores (ROC, PR, etc.) for each comparison. The final  
454 comparison between MeTeOR and a literature-derived source was calculated with a paired t-test  
455 on the group of average AUCs or PRs from the bootstraps. Any reference which had fewer than  
456 3 overlaps with either MeTeOR or a literature-derived source was discarded. Additionally,  
457 references were broken down by type if provided (example: BIOGRID High and Low  
458 Throughput).

459

460 **Box Plots and Statistics:** Boxes define the 25<sup>th</sup> -75<sup>th</sup> percentiles, with the whiskers extending  
461 from min to max, and the line in the middle defining the median. All statistical tests are two-  
462 sided. For comparisons against the ground truths in Figure 2A, all values are means of the  
463 bootstrap values, and these means were compared with a paired t-test, when all values were  
464 pooled together, they passed a D'Agostino & Pearson normality test with a K2=1.615, p=0.4459  
465 for the literature-derived source and K2=0.6366, p=0.7274 for MeTeOR.

466

467 **Data Normalization:** The MeTeOR network was smoothed using Laplacian normalization, as  
468 defined by:

$$469 \quad L = I - D^{-0.5} * A * D^{-0.5}$$

470 where L is the normalized Laplacian, D is the degree matrix, and A is the adjacency matrix of the  
471 network. This was done for each mode (gene-gene, gene-disease, gene-drug, etc.). For large-  
472 scale ranking, the absolute value of the non-diagonal elements was used. In individual rankings,  
473 such as to EGFR, the non-normalized data was used to provide easy interpretation.

474

475 **Collection of Ground Truths:** In order to determine if MeTeOR contained valid gene, disease,  
476 and drug information, ground truths were collected from the literature. MSIGDB refers to the

477 canonical pathways from MSigDB [75] and was used to determine gene-gene pathway-level  
478 associations, while the components of BIOGRID [19] represented physical gene-gene  
479 associations. A gene-gene association was made for MSIGDB if two genes were present in a  
480 pathway together, and each association was given a confidence  $\sum \frac{1}{\|Pathway\|}$  and then all  
481 confidence scores were normalized to Z-scores. The top 0.1% of associations (N=32,000) were  
482 used as a ground truth to prevent promiscuous associations.

483 There were several databases for gene-disease associations including the Comparative  
484 Toxicogenomic Database (CTD) [20] and DisGeNET [76], and these databases were broken  
485 down into their component pieces and mapped to Entrez IDs for genes and MeSH terms for  
486 diseases. For gene-drug interactions, the primary sources of data were DGIdb [77] and  
487 Drugbank, downloaded through BIOGRID [19]. Pubchem CIDs [32] were used to map MeSH  
488 chemicals [32] and Drugbank's mapping facilitated Drugbank IDs to CIDs. All STRING  
489 networks were mapped to Entrez IDs though STRING's provided mappings from STRING 9 and  
490 STRING 10. All references were retrieved in March 2018. Mappings created in this project can  
491 be found within the data repositories provided with this paper.

492

493 **Collection of Text-Mining Algorithms:** STRING-Literature (version 10.5), EVEX, STITCH-  
494 Literature (version 5), and DisGeNET's BeFree (version 5) were chosen as representative  
495 Natural Language Processing (NLP) efforts to mine gene-gene, gene-drug, and gene-disease  
496 relationships from the literature. All these efforts are publicly available and have been through  
497 multiple revisions as they undergo continued development.

498

499 **Naïve Unsupervised Prediction Methods:** Two naïve methods were used to compare against a  
500 more advanced algorithm, Non-negative Matrix Factorization (NMF). These algorithms were the  
501 Common Neighbors algorithm and the Adamic/Adar algorithms, calculated to include edge  
502 weight confidence. These were selected because of their top performance in Kastrin et al.[30].  
503 Though it is worth noting that in this publication, we include SCRs and limit the analysis to  
504 specific edge types (e.g. gene-gene), which is not true in Kastrin et al.[30].

505

506 **Non-negative Matrix Factorization (NMF):** The principle behind NMF is to create two low-  
507 dimensional matrices that, when multiplied together, approximate an original matrix [40]. These

508   matrices are called basis vectors, where the degree to which they can recapitulate the original  
509   matrix is determined by their size. The greater the size, the more features the basis vectors can  
510   capture. The basis vectors are determined through several optimization algorithms that act upon  
511   randomly initialized  $W$  and  $H$  matrices. In this work, we employed both the alternating least  
512   squares algorithm:

$$\min_{W, H \geq 0} f(W, H) = \frac{1}{2} \|A - WH\|_F^2 \quad \text{Eq. 3}$$

$$W = \text{rand}(m, k) \quad \text{Eq. 4-1}$$

$$\text{Solve for } H: W^T WH = W^T A \quad \text{Eq. 4-2}$$

$$H(H < 0) = \mathbf{0} \quad \text{Eq. 4-3}$$

$$\text{Then Solve for } W: HH^T W^T = HA^T \quad \text{Eq. 4-4}$$

$$W(W < 0) = \mathbf{0} \quad \text{Eq. 4-5}$$

513   and the multiplicative algorithm:

$$W = \text{rand}(m, k) \quad \text{Eq. 5-1}$$

$$H = \text{rand}(m, k) \quad \text{Eq. 5-2}$$

$$H = H \frac{W^T A}{W^T W H} \quad \text{Eq. 5-3}$$

$$W = W \frac{H^T A}{H^T H W} \quad \text{Eq. 5-4}$$

514  
515   NMF was executed computationally with MATLAB's Statistics Toolbox, with three repetitions  
516   of 5 iterations of the multiplicative algorithm in order to find the optimal basis initialization, then  
517   100 iterations of the alternating least squares were performed. For bulk analysis, this was done  
518   one time. For specific association predictions, like associations to EGFR, this NMF process was

519 completed five times, and then the Mean Reciprocal Rank was computed for each association  
520 across the NMF runs. This ensured that a stable answer was obtained despite the non-convex  
521 nature of NMF. The number of features (k) was selected using ten-fold cross validation of each  
522 mode of MeTeOR. The Matthew's Correlation Coefficient (MCC) was calculated and rounded to  
523 two digits of significance in order to select the lowest k with the highest MCC: 300 for gene-  
524 gene, 100 for gene-disease, and 50 for gene-drug.

525

526 **Retrospective:** Retrospective experiments were undertaken in order to determine if the  
527 information in MeTeOR through 2013 was sufficient to make accurate predictions that had yet to be  
528 discovered. The first retrospective experiment was a validation of the technique and quality of  
529 data, in that the MeTeOR network through 2013 was used to predict itself in 2018. After  
530 predictions were made on MeTeOR, all shared associations in the ground truth up to 2013 were  
531 removed, and the remaining predictions were assessed against the ground truth in the future.

532

533 **Tissue Culture and Crosslinking for IPMS:** Hela cells were grown in DMEM (Sigma) with  
534 10% FBS (Invitrogen) in 5% CO<sub>2</sub> at 37°C. 10<sup>8</sup> cells were crosslinked with formaldehyde by  
535 directly adding it to the culture medium to a final concentration of 0.5% for 8 min at 37°C. The  
536 cross-linking reaction was quenched by adding Glycine (Sigma) to a final concentration of 0.2M.  
537 Membrane proteins were extracted by re-suspending the pellet in LB1 buffer (50mMHEPES-  
538 KOH [pH 7.5], 140mMNaCl, 1mMEDTA, 10% glycerol, 0.5% NP-40, 1% Triton X-100) for 30  
539 min at 4°C. After centrifugation the supernatant containing crosslinked membrane and cytosolic  
540 proteins was used for immunoprecipitation. Immunoprecipitation and sample prep for mass  
541 spectrometry was performed as previously described [78].

542

543 **Mass Spectrometry:** Binding partners of EGFR were pulled down at different time points (2,  
544 10, 30, 120 seconds) after EGF stimulation and identified through ImmunoPrecipitation Mass  
545 Spectrometry (IPMS) in HeLa cells. Each IPMS experiment was conducted in triplicate, with  
546 one IPMS experiment conducted on non-stimulated cells to serve as a baseline. Peptides were  
547 reconstituted in 0.5% methanol, 0.1% formic acid and fractionated using a C18 (2 μm, Reprosil-  
548 Pur Basic, 6 cm x 150 μm) column with an EASY-nLC-1000 HPLC (Thermo Scientific) online  
549 with a Q-Exactive mass spectrometer (Thermo Scientific). A 75-minute gradient of 2-26%

550 acetonitrile, 0.1% formic acid at 800nl/min was used per fraction. A window of 300-1400 m/z at  
551 120k resolution,  $5 \times 10^5$  AGC, and 50ms injection time, was used for precursor selection. The  
552 top 50 most intense ions were selected for HCD fragmentation with a 5 m/z isolation window, 18  
553 sec exclusion time. RAW files were acquired with Xcalibur (Thermo) and processed with  
554 Proteome Discoverer 1.4 and MASCOT 2.4. Peptides were matched using a 20 ppm precursor  
555 tolerance window and 0.5 Da fragment threshold. Up to two missed cleavages were allowed. The  
556 data was filtered with a 1% false discovery rate by Percolator and abundances were calculated by  
557 the iBAQ algorithm. RAW files were then converted to mzXML and peptide abundances were  
558 distributed to gene products through Grouper software. Unique to gene PSMs must be  $\geq 1$ .

559

560 **Analysis of Mass Spectrometry:** All EGFR-associated proteins had their iBAQ levels  
561 normalized across time points and averaged across three biological replicates. All missing values  
562 were filled in with the minimum overall value. The amount at a given time point was calculated  
563 as a gradient relative to the previous time point. The gradient allowed the monitoring of protein  
564 changes over time, and clustering of the gradients through k-means revealed distinct patterns  
565 (Supplemental Fig. 6). Most patterns were self-consistent and showed a change at the initial time  
566 points, with little change thereafter, but the second group appeared to show random changes for  
567 proteins over all time points and may be promiscuously associated with EGFR (Supplemental  
568 Fig. 6). All proteins that changed more than 5% over the course of the experiment were  
569 considered true positives and associated with EGFR.

570

571 ***In vitro* Kinase Assay:** Two hundred fifty ng of purified recombinant EGFR-GST (Aa 668-  
572 1210, Sino Biological Inc, Beijing, P.R. China) was incubated with 100 ng of recombinant cyclin  
573 A2 or Cyclin E1 activated CDK2-GST kinase (ProQinase, Freiburg, Germany) in 20  $\mu$ l of kinase  
574 buffer (10 mM HEPES, pH 7.5, 50 mM glycerophosphate, 50 mM NaCl, 10 mM MgCl<sub>2</sub>, 10 mM  
575 MnCl<sub>2</sub>, 1mM DTT and 10  $\mu$ M ATP) for 30 min at 30°C. The reaction was terminated by  
576 addition of SDS treatment buffer, applied to 4-12 % SDS-PAGE, and immunoblotted with anti-  
577 phopho-S/T (BD Bioscience, San Jose, CA, USA), anti-EGFR, anti-CDK2, or anti-GST  
578 antibodies (Santa Cruz Biotechnology, Dallas, TX, USA).

579

580 ***In vivo* Reciprocal Pull-Down:** HEK293 cells were grown in 6 cm dishes and transfected with 2

581  $\mu$ g of WT-EGFR and WT-CDK2 expression construct using lipofectamine 2000 (Life  
582 Technologies, Carlsbad, CA. USA). After 24 h incubation at 37°C, cells were lysed with Buffer  
583 (10 mM HEPES, pH 7.5, 10 mM KCl, 0.1 mM EDTA, 1 mM DTT, 0.25% NP-40) containing  
584 protease inhibitor cocktail (Roche). Lysates were centrifuged at 6,000 rpm for 4 min and the  
585 supernatants were transferred to a new tube and protein concentration measured using Bradford  
586 assay (Bio-Rad Laboratories, CA). One hundred  $\mu$ g of cell lysate was incubated with 2.5 ug of  
587 anti-myc antibody (BioLegned, San Diego, CA, USA) or anti-CDK2 antibody (Santa Cruz  
588 Biotechnology, Dallas, TX, USA) overnight at 4°C. After further incubation with 20  $\mu$ l of  
589 protein A agarose (50% (v:v) in lysis buffer (Santa Cruz Biotechnology, Dallas, TX USA), the  
590 incubation mixture was washed three times with 1 ml lysis buffer, and twice with RIPA buffer  
591 (Boston BioProducts, MA, USA) containing protease inhibitor cocktail V (Calbiochem, CA,  
592 USA). The precipitates were re-suspended in 20  $\mu$ l of 2  $\times$  SDS sample buffer and heated at 100  
593 °C for 5 min and were applied to 4-12% SDS-PAGE followed by immunoblotting using anti  
594 EGFR, anti-CDK2, or anti-GST antibodies (Santa Cruz Biotechnology, Dallas, TX, USA).  
595 Mouse IgG antibody (Santa Cruz Biotechnology) was used as a control.

596  
597 **Co-Regulation of Genes in Cancer:** The RNASeqV2 Level 3 files of 20 TCGA cancer types  
598 (BLCA, BRCA, CESC, COAD, GBM HNSC, KIRC, KIRP, LAML, LGG LIHC, LUAD, LUSC,  
599 OV PRAD, READ, SKCM, STAD, THCA, UCEC) were downloaded from TCGA data portal  
600 (<https://tcga-data.nci.nih.gov/tcga/>) on August 19, 2015. RSEM (RNA-Seq by Expectation  
601 Maximization [79]) normalized count values of 8,768 tumor samples were used to compute  
602 Spearman's rank correlation coefficient of EGFR and all other 20,426 genes. Genes with absolute  
603 values of correlation coefficient more than 0.25 were considered to be significantly co-regulated  
604 with EGFR.

605  
606 **EGFR NMF Predictions:** Because the Non-negative Matrix Factorization (NMF) predictions  
607 are based on MeTeOR associations, the NMF MeTeOR rank was subtracted from the MeTeOR  
608 rank, to obtain a MeTeOR Difference.

609  
610 **Data and Code Availability:** All data and code from the MeTeOR network is available online at  
611 <http://meteor.lichtargelab.org/> or <http://osf.io/as865>.

612

613 **Computation:** MeTeOR was assembled in python 3 and tested using MATLAB code for  
614 comparisons on an Ubuntu computer with 64 GB RAM and 4<sup>th</sup> Gen. Intel Core i7 3.7 GHz  
615 processor.

616

## 617 **ACKNOWLEDGEMENTS**

618 The authors thank Vicky Brandt, Christie Buchovecky, Teng-Kui Hsu, Rhonald Lua, and Panos  
619 Katsonis for their discussions and general feedback on the work.

620

## 621 **AUTHOR CONTRIBUTIONS**

622 SJW conceived of the project, designed the experiments, wrote the code for the experiments, and  
623 wrote the manuscript. ADW formed the initial interest around MeSH terms, helped guide the  
624 experiments and edited the manuscript. MH helped interpret and process the IPMS experiments,  
625 which YC conducted, with YI and JQ overseeing. BKC conducted the *in vitro* and *in vivo*  
626 experiments overseen by LD. DK, CHL, AK, and BW helped with experimental design and  
627 manuscript preparation. CHL prepared the TCGA RNA-Seq data. SYK helped design and  
628 implement the website. OL oversaw all experiments and manuscript preparation.

629

## 630 **INTERESTS STATEMENT**

631 The authors have no competing interests to declare.

632

## 633 **REFERENCES**

- 634 1. Swanson DR. Medical literature as a potential source of new knowledge. Bull Med Libr  
635 Assoc. 1990;78(1):29-37. PubMed PMID: 2403828; PubMed Central PMCID:  
636 PMC225324.
- 637 2. Swanson DR. Fish oil, Raynaud's syndrome, and undiscovered public knowledge.  
638 Perspectives in biology and medicine. 1986;30(1):7-18. PubMed PMID: 3797213.
- 639 3. Wren JD, Bekeredjian R, Stewart JA, Shohet RV, Garner HR. Knowledge discovery by  
640 automated identification and ranking of implicit relationships. Bioinformatics. 2004;20(3):389-  
641 98. Epub 2004/02/13. doi: 10.1093/bioinformatics/btg421. PubMed PMID: 14960466.
- 642 4. Hristovski D, Stare J, Peterlin B, Dzeroski S. Supporting discovery in medicine by  
643 association rule mining in Medline and UMLS. Studies in health technology and informatics.  
644 2001;84(Pt 2):1344-8. Epub 2001/10/18. PubMed PMID: 11604946.

645 5. Hristovski D, Kastrin A, Dinevski D, Burgun A, Ziberna L, Rindflesch TC. Using  
646 Literature-Based Discovery to Explain Adverse Drug Effects. *Journal of medical systems*.  
647 2016;40(8):185. Epub 2016/06/20. doi: 10.1007/s10916-016-0544-z. PubMed PMID: 27318993.

648 6. Weeber M, Klein H, Aronson AR, Mork JG, de Jong-van den Berg LT, Vos R. Text-  
649 based discovery in biomedicine: the architecture of the DAD-system. *Proceedings / AMIA*  
650 Annual Symposium AMIA Symposium. 2000:903-7. PubMed PMID: 11080015; PubMed  
651 Central PMCID: PMC2243779.

652 7. Torvik VI, Smalheiser NR. A quantitative model for linking two disparate sets of articles  
653 in MEDLINE. *Bioinformatics*. 2007;23(13):1658-65. doi: 10.1093/bioinformatics/btm161.  
654 PubMed PMID: 17463015.

655 8. Stegmann J, Grohmann G. Hypothesis generation guided by co-word clustering.  
656 *Scientometrics*. 2003;56(1):111-35.

657 9. Katukuri JR, Xie Y, Raghavan VV, Gupta A. Hypotheses generation as supervised link  
658 discovery with automated class labeling on large-scale biomedical concept networks. *BMC*  
659 *genomics*. 2012;13 Suppl 3:S5. doi: 10.1186/1471-2164-13-S3-S5. PubMed PMID: 22759614;  
660 PubMed Central PMCID: PMC3394427.

661 10. Cameron D, Bodenreider O, Yalamanchili H, Danh T, Vallabhaneni S, Thirunarayan K,  
662 et al. A graph-based recovery and decomposition of Swanson's hypothesis using semantic  
663 predication. *Journal of biomedical informatics*. 2013;46(2):238-51. doi:  
664 10.1016/j.jbi.2012.09.004. PubMed PMID: 23026233; PubMed Central PMCID: PMC4031661.

665 11. Hristovski D, Friedman C, Rindflesch TC, Peterlin B. Exploiting semantic relations for  
666 literature-based discovery. *AMIA Annu Symp Proc*. 2006:349-53. Epub 2007/01/24. PubMed  
667 PMID: 17238361; PubMed Central PMCID: PMCPMC1839258.

668 12. Gordon MD, Lindsay RK. Toward discovery support systems: A replication,  
669 re-examination, and extension of Swanson's work on literature-based discovery of a connection  
670 between Raynaud's and fish oil. *Journal of the American Society for Information Science*.  
671 1996;47(2):116-28.

672 13. Vlasblom J, Zuberi K, Rodriguez H, Arnold R, Gagarinova A, Deineko V, et al. Novel  
673 function discovery with GeneMANIA: a new integrated resource for gene function prediction in  
674 *Escherichia coli*. *Bioinformatics*. 2015;31(3):306-10. doi: 10.1093/bioinformatics/btu671.  
675 PubMed PMID: 25316676; PubMed Central PMCID: PMCPMC4308668.

676 14. International Multiple Sclerosis Genetics C. Network-based multiple sclerosis pathway  
677 analysis with GWAS data from 15,000 cases and 30,000 controls. *American journal of human*  
678 *genetics*. 2013;92(6):854-65. doi: 10.1016/j.ajhg.2013.04.019. PubMed PMID: 23731539;  
679 PubMed Central PMCID: PMCPMC3958952.

680 15. Lim J, Hao T, Shaw C, Patel AJ, Szabo G, Rual JF, et al. A protein-protein interaction  
681 network for human inherited ataxias and disorders of Purkinje cell degeneration. *Cell*.  
682 2006;125(4):801-14. doi: 10.1016/j.cell.2006.03.032. PubMed PMID: 16713569.

683 16. Pujana MA, Han JD, Starita LM, Stevens KN, Tewari M, Ahn JS, et al. Network  
684 modeling links breast cancer susceptibility and centrosome dysfunction. *Nature genetics*.  
685 2007;39(11):1338-49. doi: 10.1038/ng.2007.2. PubMed PMID: 17922014.

686 17. Chuang HY, Lee E, Liu YT, Lee D, Ideker T. Network-based classification of breast  
687 cancer metastasis. *Molecular systems biology*. 2007;3:140. doi: 10.1038/msb4100180. PubMed  
688 PMID: 17940530; PubMed Central PMCID: PMCPMC2063581.

689 18. Hofree M, Shen JP, Carter H, Gross A, Ideker T. Network-based stratification of tumor  
690 mutations. *Nature methods*. 2013;10(11):1108-15. doi: 10.1038/nmeth.2651. PubMed PMID:  
691 24037242; PubMed Central PMCID: PMC3866081.

692 19. Chatr-Aryamontri A, Breitkreutz BJ, Heinicke S, Boucher L, Winter A, Stark C, et al.  
693 The BioGRID interaction database: 2013 update. *Nucleic acids research*. 2013;41(Database  
694 issue):D816-23. doi: 10.1093/nar/gks1158. PubMed PMID: 23203989; PubMed Central PMCID:  
695 PMC3531226.

696 20. Davis AP, Grondin CJ, Lennon-Hopkins K, Saraceni-Richards C, Sciaky D, King BL, et  
697 al. The Comparative Toxicogenomics Database's 10th year anniversary: update 2015. *Nucleic  
698 acids research*. 2014. doi: 10.1093/nar/gku935. PubMed PMID: 25326323.

699 21. Davis AP, Wiegers TC, Roberts PM, King BL, Lay JM, Lennon-Hopkins K, et al. A  
700 CTD-Pfizer collaboration: manual curation of 88,000 scientific articles text mined for drug-  
701 disease and drug-phenotype interactions. *Database : the journal of biological databases and  
702 curation*. 2013;2013:bat080. doi: 10.1093/database/bat080. PubMed PMID: 24288140; PubMed  
703 Central PMCID: PMC3842776.

704 22. Van Landeghem S, Bjorne J, Wei CH, Hakala K, Pyysalo S, Ananiadou S, et al. Large-  
705 scale event extraction from literature with multi-level gene normalization. *PloS one*.  
706 2013;8(4):e55814. doi: 10.1371/journal.pone.0055814. PubMed PMID: 23613707; PubMed  
707 Central PMCID: PMCPMC3629104.

708 23. Hirschberg J, Manning CD. Advances in natural language processing. *Science*.  
709 2015;349(6245):261-6. doi: 10.1126/science.aaa8685. PubMed PMID: 26185244.

710 24. Mallory EK, Zhang C, Re C, Altman RB. Large-scale extraction of gene interactions  
711 from full-text literature using DeepDive. *Bioinformatics*. 2016;32(1):106-13. doi:  
712 10.1093/bioinformatics/btv476. PubMed PMID: 26338771; PubMed Central PMCID:  
713 PMCPMC4681986.

714 25. Arighi CN, Lu Z, Krallinger M, Cohen KB, Wilbur WJ, Valencia A, et al. Overview of  
715 the BioCreative III Workshop. *BMC Bioinformatics*. 2011;12 Suppl 8:S1. Epub 2011/12/22. doi:  
716 10.1186/1471-2105-12-S8-S1. PubMed PMID: 22151647; PubMed Central PMCID:  
717 PMCPMC3269932.

718 26. Minguet F, Salgado TM, van den Boogerd L, Fernandez-Llimos F. Quality of pharmacy-  
719 specific Medical Subject Headings (MeSH) assignment in pharmacy journals indexed in  
720 MEDLINE. *Res Social Adm Pharm*. 2015;11(5):686-95. doi: 10.1016/j.sapharm.2014.11.004.  
721 PubMed PMID: 25498253.

722 27. Karic A, Karic A. Using the BITOLA system to identify candidate genes for Parkinson's  
723 disease. *Bosnian journal of basic medical sciences*. 2011;11(3):185-9. Epub 2011/08/31. doi:  
724 10.17305/bjbms.2011.2572. PubMed PMID: 21875422; PubMed Central PMCID:  
725 PMCPMC4362554.

726 28. Hristovski D, Peterlin B, Mitchell JA, Humphrey SM, Sitbon L, Turner I. Improving  
727 literature based discovery support by genetic knowledge integration. *Studies in health technology  
728 and informatics*. 2003;95.

729 29. Srinivasan P. Text mining: generating hypotheses from MEDLINE. *Journal of the  
730 American Society for Information Science and Technology*. 2004;55(5):396-413.

731 30. Kastrin A, Rindflesch TC, Hristovski D. Link Prediction on a Network of Co-occurring  
732 MeSH Terms: Towards Literature-based Discovery. *Methods Inf Med*. 2016;55(4):340-6. doi:  
733 10.3414/ME15-01-0108. PubMed PMID: 27435341.

734 31. Gray KA, Yates B, Seal RL, Wright MW, Bruford EA. Genenames.org: the HGNC  
735 resources in 2015. *Nucleic acids research*. 2015;43(Database issue):D1079-85. doi:  
736 10.1093/nar/gku1071. PubMed PMID: 25361968.

737 32. Kim S, Thiessen PA, Bolton EE, Chen J, Fu G, Gindulyte A, et al. PubChem Substance  
738 and Compound databases. *Nucleic acids research*. 2016;44(D1):D1202-13. doi:  
739 10.1093/nar/gkv951. PubMed PMID: 26400175.

740 33. Alstott J, Bullmore E, Plenz D. Powerlaw: a Python package for analysis of heavy-tailed  
741 distributions. *PloS one*. 2014;9(1):e85777. doi: 10.1371/journal.pone.0085777. PubMed PMID:  
742 24489671; PubMed Central PMCID: PMCPMC3906378.

743 34. Barabasi AL, Albert R. Emergence of scaling in random networks. *Science*.  
744 1999;286(5439):509-12. PubMed PMID: 10521342.

745 35. Szklarczyk D, Franceschini A, Wyder S, Forsslund K, Heller D, Huerta-Cepas J, et al.  
746 STRING v10: protein-protein interaction networks, integrated over the tree of life. *Nucleic acids  
747 research*. 2015;43(Database issue):D447-52. doi: 10.1093/nar/gku1003. PubMed PMID:  
748 25352553; PubMed Central PMCID: PMCPMC4383874.

749 36. Bravo A, Pinero J, Queralt-Rosinach N, Rautschka M, Furlong LI. Extraction of relations  
750 between genes and diseases from text and large-scale data analysis: implications for translational  
751 research. *BMC bioinformatics*. 2015;16:55. doi: 10.1186/s12859-015-0472-9. PubMed PMID:  
752 25886734; PubMed Central PMCID: PMCPMC4466840.

753 37. Szklarczyk D, Santos A, von Mering C, Jensen LJ, Bork P, Kuhn M. STITCH 5:  
754 augmenting protein-chemical interaction networks with tissue and affinity data. *Nucleic acids  
755 research*. 2016;44(D1):D380-4. doi: 10.1093/nar/gkv1277. PubMed PMID: 26590256; PubMed  
756 Central PMCID: PMCPMC4702904.

757 38. Kim H, Park H, Drake BL. Extracting unrecognized gene relationships from the  
758 biomedical literature via matrix factorizations. *BMC bioinformatics*. 2007;8 Suppl 9:S6. doi:  
759 10.1186/1471-2105-8-S9-S6. PubMed PMID: 18047707; PubMed Central PMCID:  
760 PMC2217664.

761 39. Spangler S, Wilkins AD, Bachman BJ, Nagarajan M, Dayaram T, Haas P, et al., editors.  
762 Automated hypothesis generation based on mining scientific literature. *Proceedings of the 20th  
763 ACM SIGKDD international conference on Knowledge discovery and data mining*; 2014: ACM.

764 40. Koren Y, Bell R, Volinsky C. Matrix factorization techniques for recommender systems.  
765 *Computer*. 2009;(8):30-7.

766 41. Sun J, Ting MC, Ishii M, Maxson R. Msx1 and Msx2 function together in the regulation  
767 of primordial germ cell migration in the mouse. *Dev Biol*. 2016;417(1):11-24. Epub 2016/07/21.  
768 doi: 10.1016/j.ydbio.2016.07.013. PubMed PMID: 27435625; PubMed Central PMCID:  
769 PMCPMC5407493.

770 42. DeParis SW, Bloomer M, Han Y, Vagefi MR, Shieh JTC, Solomon DA, et al. Uveal  
771 Ganglioneuroma due to Germline PTEN Mutation (Cowden Syndrome) Presenting as Unilateral  
772 Infantile Glaucoma. *Ocular oncology and pathology*. 2017;3(2):122-8. Epub 2017/09/05. doi:  
773 10.1159/000450552. PubMed PMID: 28868283; PubMed Central PMCID: PMCPMC5566766.

774 43. Lascaratos G, Chau KY, Zhu H, Gkotsi D, Kamal D, Gout I, et al. Systemic PTEN-Akt1-  
775 mTOR pathway activity in patients with normal tension glaucoma and ocular hypertension: A  
776 case series. *Mitochondrion*. 2017;36:96-102. Epub 2017/05/14. doi: 10.1016/j.mito.2017.05.003.  
777 PubMed PMID: 28499984.

778 44. Lazzari E, Mondala PK, Santos ND, Miller AC, Pineda G, Jiang Q, et al. Alu-dependent  
779 RNA editing of GLI1 promotes malignant regeneration in multiple myeloma. *Nature*

780 communications. 2017;8(1):1922. doi: 10.1038/s41467-017-01890-w. PubMed PMID:  
781 29203771; PubMed Central PMCID: PMCPMC5715072.

782 45. Hazenberg MD, Otto SA, Hamann D, Roos MT, Schuitemaker H, de Boer RJ, et al.  
783 Depletion of naive CD4 T cells by CXCR4-using HIV-1 variants occurs mainly through  
784 increased T-cell death and activation. AIDS (London, England). 2003;17(10):1419-24. Epub  
785 2003/06/26. doi: 10.1097/01.aids.0000072661.21517.fl. PubMed PMID: 12824778.

786 46. Cheever MA, Allison JP, Ferris AS, Finn OJ, Hastings BM, Hecht TT, et al. The  
787 prioritization of cancer antigens: a national cancer institute pilot project for the acceleration of  
788 translational research. Clin Cancer Res. 2009;15(17):5323-37. Epub 2009/09/03. doi:  
789 10.1158/1078-0432.CCR-09-0737. PubMed PMID: 19723653; PubMed Central PMCID:  
790 PMCPMC5779623.

791 47. Maslak PG, Dao T, Bernal Y, Chanel SM, Zhang R, Frattini M, et al. Phase 2 trial of a  
792 multivalent WT1 peptide vaccine (galinpepimut-S) in acute myeloid leukemia. Blood Adv.  
793 2018;2(3):224-34. Epub 2018/02/02. doi: 10.1182/bloodadvances.2017014175. PubMed PMID:  
794 29386195; PubMed Central PMCID: PMCPMC5812332.

795 48. Hanahan D, Weinberg RA. Hallmarks of cancer: the next generation. Cell.  
796 2011;144(5):646-74. doi: 10.1016/j.cell.2011.02.013. PubMed PMID: 21376230.

797 49. von Mering C, Jensen LJ, Snel B, Hooper SD, Krupp M, Foglierini M, et al. STRING:  
798 known and predicted protein-protein associations, integrated and transferred across organisms.  
799 Nucleic acids research. 2005;33(Database issue):D433-7. doi: 10.1093/nar/gki005. PubMed  
800 PMID: 15608232; PubMed Central PMCID: PMCPMC539959.

801 50. Tomczak K, Czerwinska P, Wiznerowicz M. The Cancer Genome Atlas (TCGA): an  
802 immeasurable source of knowledge. Contemp Oncol (Pozn). 2015;19(1A):A68-77. doi:  
803 10.5114/wo.2014.47136. PubMed PMID: 25691825; PubMed Central PMCID:  
804 PMCPMC4322527.

805 51. Goos JA, Hiemstra AC, Coupe VM, Diosdado B, Kooijman W, Delis-Van Diemen PM,  
806 et al. Epidermal growth factor receptor (EGFR) and prostaglandin-endoperoxide synthase 2  
807 (PTGS2) are prognostic biomarkers for patients with resected colorectal cancer liver metastases.  
808 Br J Cancer. 2014;111(4):749-55. doi: 10.1038/bjc.2014.354. PubMed PMID: 24983372;  
809 PubMed Central PMCID: PMCPMC4134500.

810 52. Hsu JY, Chang KY, Chen SH, Lee CT, Chang ST, Cheng HC, et al. Epidermal growth  
811 factor-induced cyclooxygenase-2 enhances head and neck squamous cell carcinoma metastasis  
812 through fibronectin up-regulation. Oncotarget. 2015;6(3):1723-39. doi:  
813 10.18632/oncotarget.2783. PubMed PMID: 25595899; PubMed Central PMCID:  
814 PMCPMC4359327.

815 53. Li H, Wang Y, Su F, Li J, Gong P. Monitoring of cyclooxygenase-2 levels can predict  
816 EGFR mutations and the efficacy of EGFR-TKI in patients with lung adenocarcinoma. Int J Clin  
817 Exp Pathol. 2015;8(5):5577-83. PubMed PMID: 26191267; PubMed Central PMCID:  
818 PMCPMC4503138.

819 54. Wang L, Hu H, Pan Y, Wang R, Li Y, Shen L, et al. PIK3CA mutations frequently  
820 coexist with EGFR/KRAS mutations in non-small cell lung cancer and suggest poor prognosis in  
821 EGFR/KRAS wildtype subgroup. PloS one. 2014;9(2):e88291. doi:  
822 10.1371/journal.pone.0088291. PubMed PMID: 24533074; PubMed Central PMCID:  
823 PMCPMC3922761.

824 55. Foerster S, Kacprowski T, Dhople VM, Hammer E, Herzog S, Saafan H, et al.  
825 Characterization of the EGFR interactome reveals associated protein complex networks and

826 intracellular receptor dynamics. *Proteomics*. 2013;13(21):3131-44. doi:  
827 10.1002/pmic.201300154. PubMed PMID: 23956138.

828 56. Jones RB, Gordus A, Krall JA, MacBeath G. A quantitative protein interaction network  
829 for the ErbB receptors using protein microarrays. *Nature*. 2006;439(7073):168-74. doi:  
830 10.1038/nature04177. PubMed PMID: 16273093.

831 57. Li J, Bennett K, Stukalov A, Fang B, Zhang G, Yoshida T, et al. Perturbation of the  
832 mutated EGFR interactome identifies vulnerabilities and resistance mechanisms. *Molecular  
833 systems biology*. 2013;9:705. doi: 10.1038/msb.2013.61. PubMed PMID: 24189400; PubMed  
834 Central PMCID: PMCPMC4039310.

835 58. Simper NB, Jones CL, MacLennan GT, Montironi R, Williamson SR, Osunkoya AO, et  
836 al. Basal cell carcinoma of the prostate is an aggressive tumor with frequent loss of PTEN  
837 expression and overexpression of EGFR. *Human pathology*. 2015;46(6):805-12. Epub  
838 2015/04/15. doi: 10.1016/j.humpath.2015.02.004. PubMed PMID: 25870120.

839 59. Davis NM, Sokolosky M, Stadelman K, Abrams SL, Libra M, Candido S, et al.  
840 Deregulation of the EGFR/PI3K/PTEN/Akt/mTORC1 pathway in breast cancer: possibilities for  
841 therapeutic intervention. *Oncotarget*. 2014;5(13):4603-50. Epub 2014/07/23. doi:  
842 10.18632/oncotarget.2209. PubMed PMID: 25051360; PubMed Central PMCID:  
843 PMCPMC4148087.

844 60. Kuppuswamy D, Dalton M, Pike LJ. Serine 1002 is a site of in vivo and in vitro  
845 phosphorylation of the epidermal growth factor receptor. *The Journal of biological chemistry*.  
846 1993;268(25):19134-42. PubMed PMID: 8360196.

847 61. Hiromura K, Pippin JW, Blonski MJ, Roberts JM, Shankland SJ. The subcellular  
848 localization of cyclin dependent kinase 2 determines the fate of mesangial cells: role in apoptosis  
849 and proliferation. *Oncogene*. 2002;21(11):1750-8. doi: 10.1038/sj.onc.1205238. PubMed PMID:  
850 11896606.

851 62. Yoshida A, Yoneda-Kato N, Kato JY. CSN5 specifically interacts with CDK2 and  
852 controls senescence in a cytoplasmic cyclin E-mediated manner. *Scientific reports*. 2013;3:1054.  
853 doi: 10.1038/srep01054. PubMed PMID: 23316279; PubMed Central PMCID:  
854 PMCPMC3542532.

855 63. Xue Y, Ren J, Gao X, Jin C, Wen L, Yao X. GPS 2.0, a tool to predict kinase-specific  
856 phosphorylation sites in hierarchy. *Molecular & cellular proteomics : MCP*. 2008;7(9):1598-608.  
857 doi: 10.1074/mcp.M700574-MCP200. PubMed PMID: 18463090; PubMed Central PMCID:  
858 PMCPMC2528073.

859 64. Nickerson RS. Confirmation bias: A ubiquitous phenomenon in many guises. *Review of  
860 general psychology*. 1998;2(2):175.

861 65. Lee MD, Navarro DJ, Nikkerud H, editors. *An empirical evaluation of models of text  
862 document similarity*. Proceedings of the Cognitive Science Society; 2005.

863 66. Chohan TA, Qian H, Pan Y, Chen JZ. Cyclin-dependent kinase-2 as a target for cancer  
864 therapy: progress in the development of CDK2 inhibitors as anti-cancer agents. *Current  
865 medicinal chemistry*. 2015;22(2):237-63. PubMed PMID: 25386824.

866 67. Zhai H, Zhong W, Yang X, Wu YL. Neoadjuvant and adjuvant epidermal growth factor  
867 receptor tyrosine kinase inhibitor (EGFR-TKI) therapy for lung cancer. *Transl Lung Cancer Res*.  
868 2015;4(1):82-93. doi: 10.3978/j.issn.2218-6751.2014.11.08. PubMed PMID: 25806348; PubMed  
869 Central PMCID: PMCPMC4367710.

870 68. Kumar A, Petri ET, Halmos B, Boggon TJ. Structure and clinical relevance of the  
871 epidermal growth factor receptor in human cancer. *J Clin Oncol*. 2008;26(10):1742-51. doi:

872 10.1200/JCO.2007.12.1178. PubMed PMID: 18375904; PubMed Central PMCID:  
873 PMC3799959.

874 69. Yamasaki F, Zhang D, Bartholomeusz C, Sudo T, Hortobagyi GN, Kurisu K, et al.  
875 Sensitivity of breast cancer cells to erlotinib depends on cyclin-dependent kinase 2 activity. Mol  
876 Cancer Ther. 2007;6(8):2168-77. doi: 10.1158/1535-7163.MCT-06-0514. PubMed PMID:  
877 17671085; PubMed Central PMCID: PMC2603172.

878 70. MeSH Browser: National Library of Medicine; 2017. Available from:  
879 <https://meshb.nlm.nih.gov>.

880 71. Rindflesch TC, Fiszman M. The interaction of domain knowledge and linguistic structure  
881 in natural language processing: interpreting hypernymic propositions in biomedical text. Journal  
882 of biomedical informatics. 2003;36(6):462-77.

883 72. PhySH - Physics Subject Headings: American Physical Society; 2017 [cited 2017  
884 8/14/17]. Available from: <https://physh.aps.org/>.

885 73. Gramatica R, Di Matteo T, Giorgetti S, Barbiani M, Bevec D, Aste T. Graph theory  
886 enables drug repurposing--how a mathematical model can drive the discovery of hidden  
887 mechanisms of action. PloS one. 2014;9(1):e84912. doi: 10.1371/journal.pone.0084912. PubMed  
888 PMID: 24416311; PubMed Central PMCID: PMC3886994.

889 74. Liekens AM, De Knijf J, Daelemans W, Goethals B, De Rijk P, Del-Favero J. BioGraph:  
890 unsupervised biomedical knowledge discovery via automated hypothesis generation. Genome  
891 biology. 2011;12(6):R57. doi: 10.1186/gb-2011-12-6-r57. PubMed PMID: 21696594; PubMed  
892 Central PMCID: PMC3218845.

893 75. Liberzon A, Birger C, Thorvaldsdottir H, Ghandi M, Mesirov JP, Tamayo P. The  
894 Molecular Signatures Database (MSigDB) hallmark gene set collection. Cell Syst.  
895 2015;1(6):417-25. doi: 10.1016/j.cels.2015.12.004. PubMed PMID: 26771021; PubMed Central  
896 PMCID: PMC4707969.

897 76. Pinero J, Queralt-Rosinach N, Bravo A, Deu-Pons J, Bauer-Mehren A, Baron M, et al.  
898 DisGeNET: a discovery platform for the dynamical exploration of human diseases and their  
899 genes. Database : the journal of biological databases and curation. 2015;2015:bav028. Epub  
900 2015/04/17. doi: 10.1093/database/bav028. PubMed PMID: 25877637; PubMed Central  
901 PMCID: PMC4397996.

902 77. Griffith M, Griffith OL, Coffman AC, Weible JV, McMichael JF, Spies NC, et al.  
903 DGIdb: mining the druggable genome. Nature methods. 2013;10(12):1209-10. doi:  
904 10.1038/nmeth.2689. PubMed PMID: 24122041; PubMed Central PMCID: PMC3851581.

905 78. Malovannaya A, Li Y, Bulynko Y, Jung SY, Wang Y, Lanz RB, et al. Streamlined  
906 analysis schema for high-throughput identification of endogenous protein complexes.  
907 Proceedings of the National Academy of Sciences of the United States of America.  
908 2010;107(6):2431-6. doi: 10.1073/pnas.0912599106. PubMed PMID: 20133760; PubMed  
909 Central PMCID: PMC2823922.

910 79. Li B, Ruotti V, Stewart RM, Thomson JA, Dewey CN. RNA-Seq gene expression  
911 estimation with read mapping uncertainty. Bioinformatics. 2010;26(4):493-500. doi:  
912 10.1093/bioinformatics/btp692. PubMed PMID: 20022975; PubMed Central PMCID:  
913 PMC2820677.

914

# Wilson - Figure 1

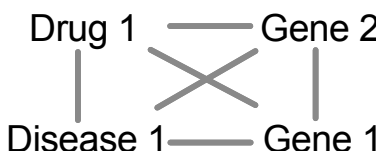
## a Extract Terms



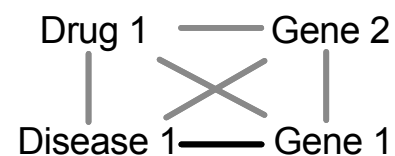
Article 1

Disease 1  
Drug 1  
Gene 1  
Gene 2

## Connect Terms

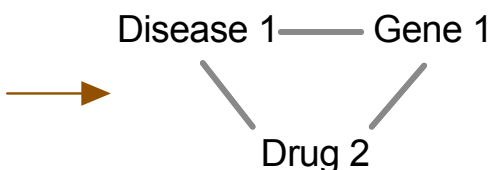


## Merge Terms



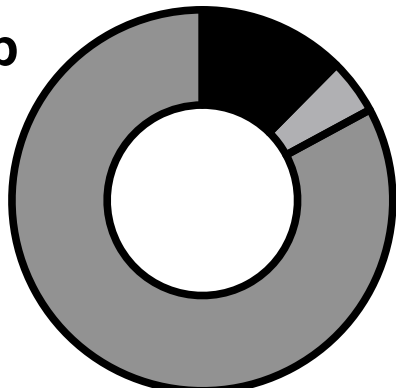
1 Article

> 1 Article



Article 2  $\times 10^{10}$

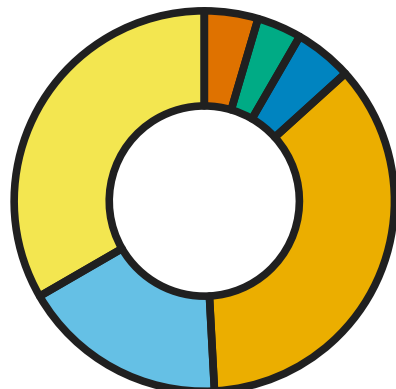
## b



### Nodes

- 12.4% Genes
- 4.7% Diseases
- 82.9% Drugs

Total= $1.07 \times 10^5$

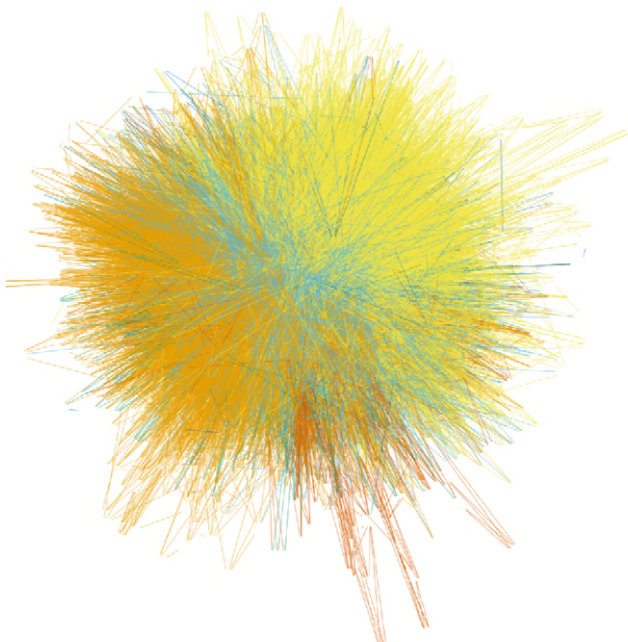


### Edges

- 4.6% Gene-Gene
- 3.8% Gene-Drug
- 4.9% Gene-Disease
- 35.9% Drug-Drug
- 17.5% Drug-Disease
- 33.3% Disease-Disease

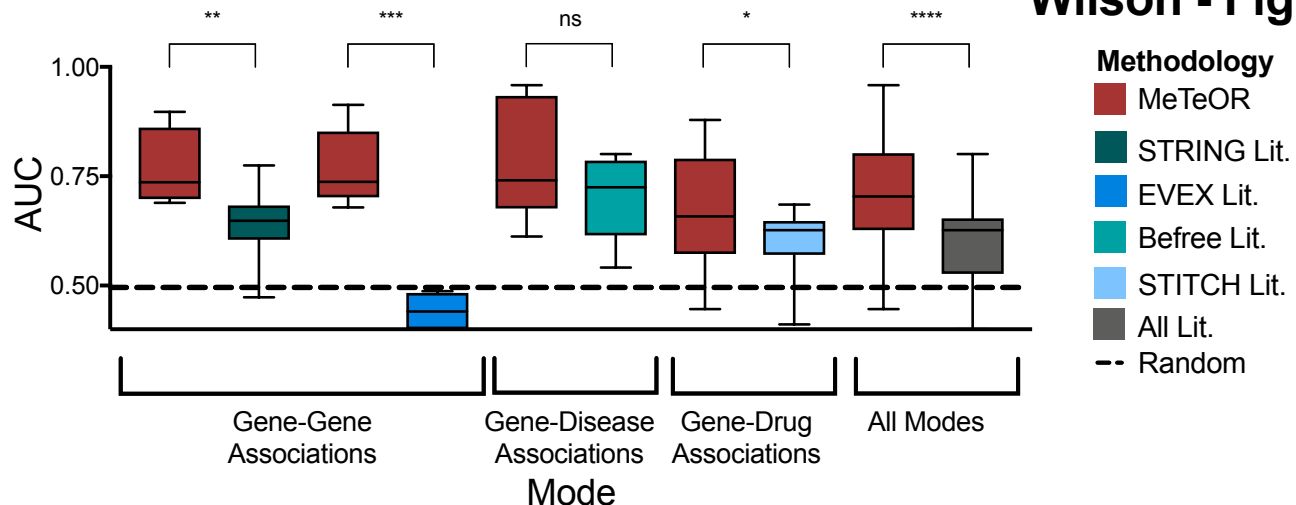
Total= $9.01 \times 10^6$

## c

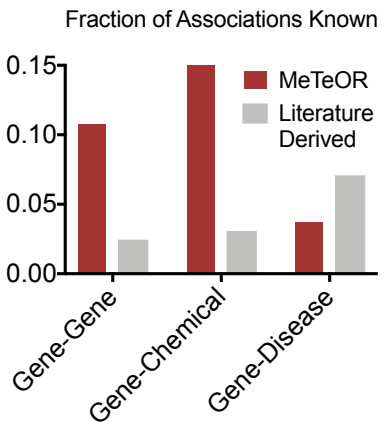


# Wilson - Figure 2

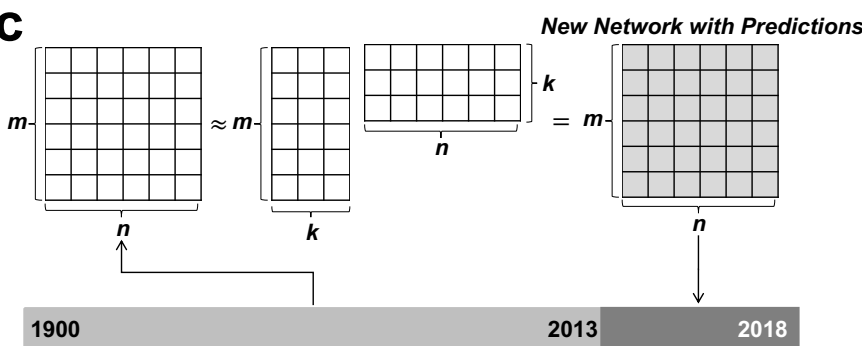
**a**



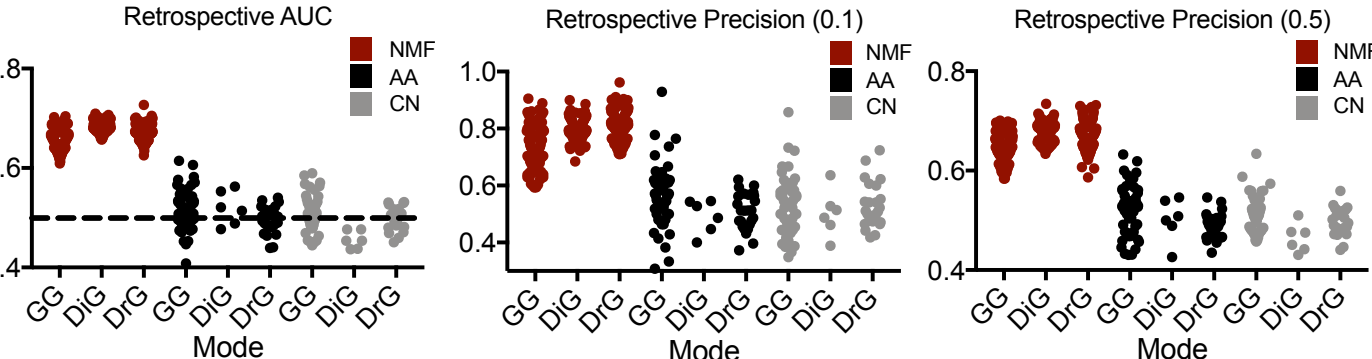
**b**



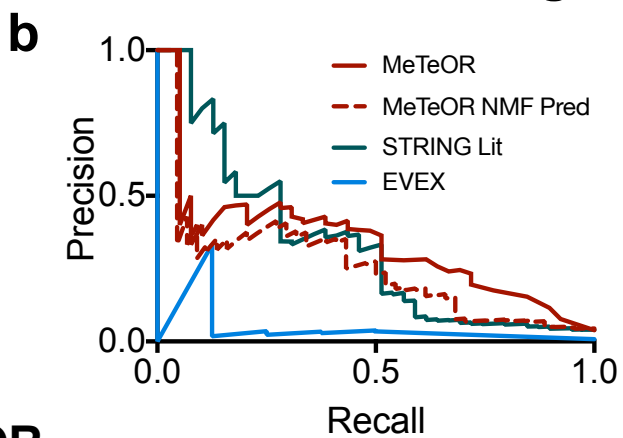
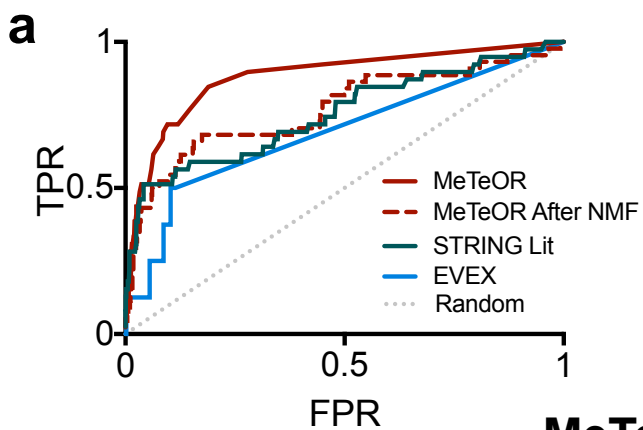
**c**



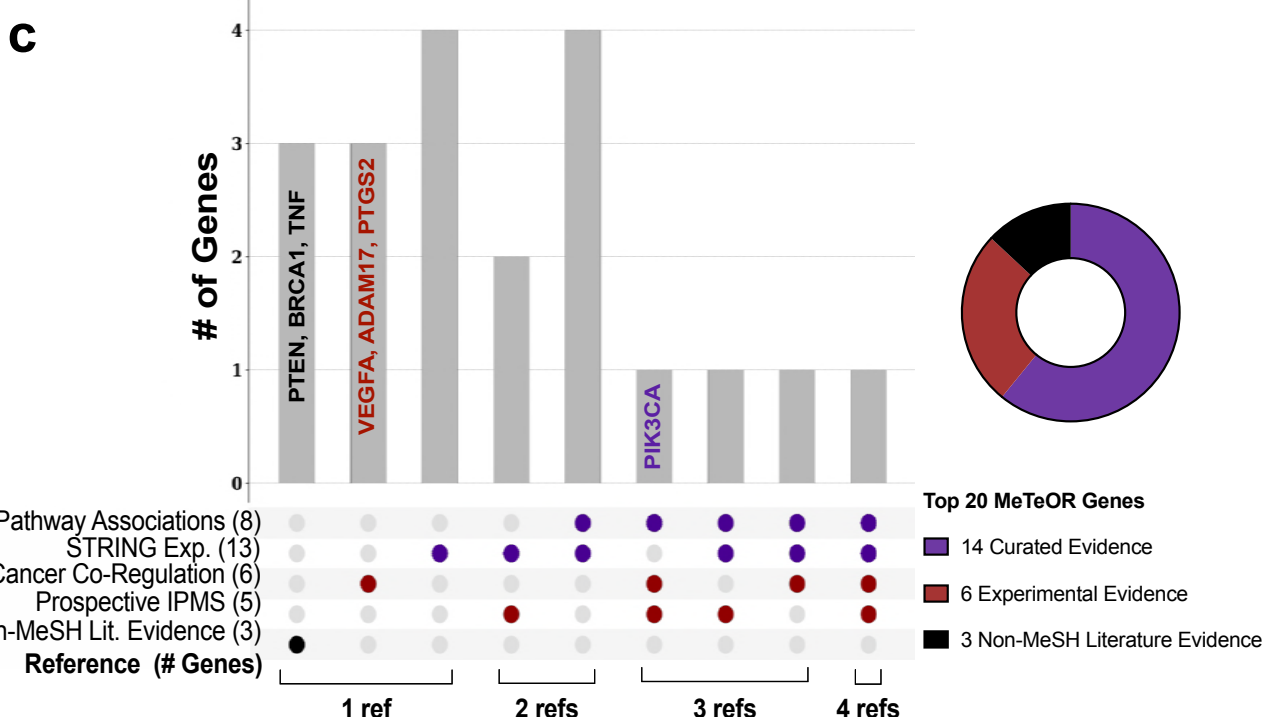
**d**



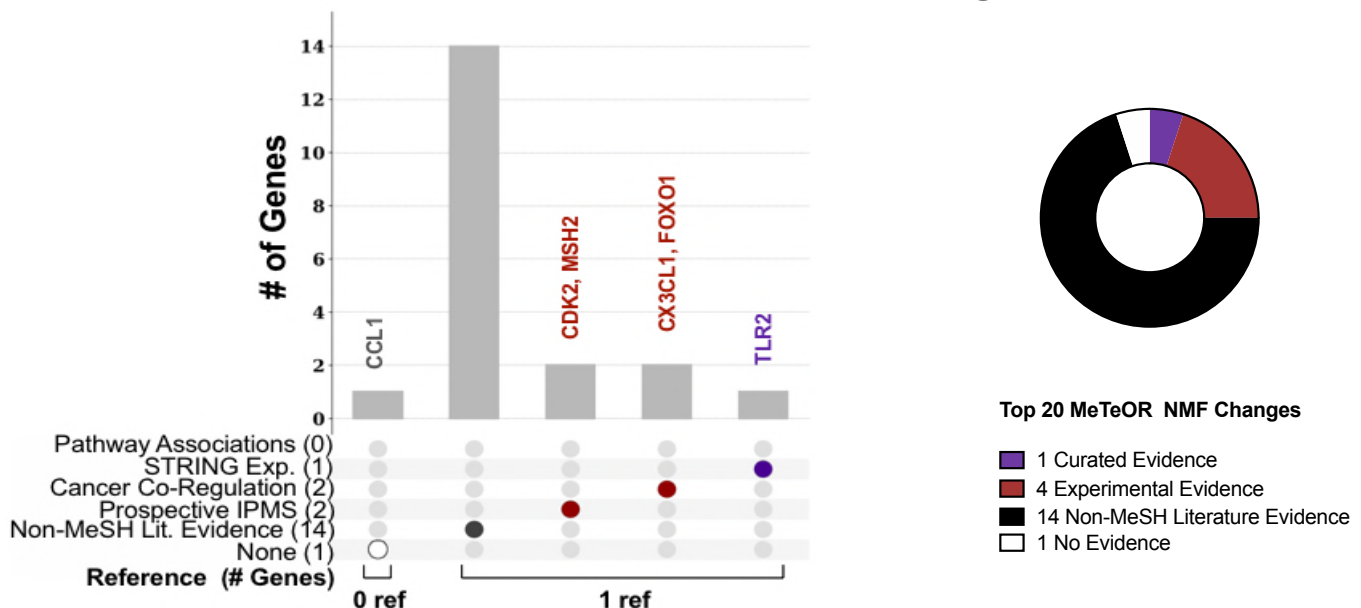
# Wilson - Figure 3



## MeTeOR



## MeTeOR NMF Rank Change



# Wilson - Figure 4

